

Distributionally Robust Airport Ground Holding Problem under Wasserstein Ambiguity Sets

Haochen Wu*, Alexander S. Estes[†], Max Z. Li[‡]

Abstract

Ground Delay Programs (GDPs) mitigate demand–capacity imbalances by holding flights on the ground when an airport’s arrival capacity is reduced, thereby reducing costly airborne holding. A central challenge is that day-to-day demand–capacity balancing relies on accurate predictions of airport capacities. However, these predictions are deeply uncertain: forecast errors, operational disruptions, and climate change–driven shifts in weather severity can induce distribution shifts in capacity outcomes. Thus, policies optimized for a single predicted distribution may be brittle out of sample.

We address this challenge by developing a *distributionally robust* framework for the single airport ground holding problem (dr-SAGHP). We also propose a method integrates Kelly’s cutting plane method with the integer L-shaped method, and that is applicable more broadly to two-stage distributionally robust integer programs with relatively complete recourse and continuous second-stage decision variables. Our method includes a novel dual bisection and primal recovery algorithm that makes use of the structure of the distributionally robust integer program in order to quickly generate subgradients required by Kelly’s cutting plane method. In computational experiments, our proposed algorithm delivers up to two orders-of-magnitude speedups compared to solving the convex reformulation directly, while maintaining negligible optimality gaps.

We generate capacity scenarios via Gaussian process regression and evaluate out-of-sample performance by perturbing the posterior mean and variance. The numerical experiment results show that dr-SAGHP delivers significant out-of-sample gains under moderate-to-severe shifts, improving the resilience and effectiveness of GDP decision-making under capacity uncertainty.

Funding:

he NASA University Leadership initiative (grant #80NSSC24M0068) provided funds to assist the authors with their research, but this article solely reflects the opinions and conclusions of its authors.

Keywords:

Distributionally Robust Optimization, Stochastic Programming, Ground Delay Program, Air Traffic Management

1 Introduction

Demand–capacity imbalances in the air transportation system are a major operational challenge with significant negative impacts on airlines, passengers, and the environment. There are a variety of potential bottlenecks within the air transportation system, with airport arrival and departure capacities being major components [Neufville et al., 2013]. Typically, if airport capacity constraints can be identified proactively, air traffic managers prefer to delay flights before they are airborne, as airborne delay costs typically drastically outweigh delay costs incurred on the ground Vranas et al. [1994]. Within the U.S. National Airspace System (NAS), such demand–capacity balancing actions take the form of Traffic Management Initiatives (TMIs) known as Ground Delay Programs (GDPs) [FAA, 2009].

However, the efficacy of these strategies is increasingly challenged by shifting environmental baselines that disrupt traditional capacity predictions. This shift is driven by the fact that climate change is not only an outcome of aviation activity, but also a driver of operational risk that aviation must

*Department of Aerospace Engineering, University of Michigan, Ann Arbor, MI, USA haocwu@umich.edu

[†]Institute for Systems Research, Department of Decisions, Operations, and Information Technology, University of Maryland, College Park, MD, USA aestes@umd.edu

[‡]Department of Aerospace Engineering, Department of Civil and Environmental Engineering, Department of Industrial and Operations Engineering, University of Michigan, Ann Arbor, MI, USA maxzli@umich.edu

adapt to [Ryley et al., 2020]. Climate change is expected to influence aviation through changes in temperature and precipitation patterns, sea-level rise, wind changes, and the impacts of more frequent and/or more intense extreme weather events [Ryley et al., 2020]. These hazards can directly affect airport and air traffic management performance via runway configuration changes, convective and storm-related constraints, and disruption from heavy precipitation and flooding, all of which translate into time-varying, uncertain airport capacities. In this sense, climate change can amplify both the frequency and the complexity of weather-driven capacity shortfalls, strengthening the need for decision models that remain reliable under imperfect predictive information.

Given known parameters such as airport capacities, nominal flight times between airports, and flight schedule information, the family of optimization models known as *Ground Holding Problems* (GHPs) can be solved to obtain optimal rescheduling decisions to minimize incurred airborne and ground delay costs [Vranas et al., 1994].

Previous works have addressed the formulation of both single airport and multi-airport variants of GHPs, referred to as the Single Airport Ground Holding Problem (SAGHP) and Multi-Airport Ground Holding Problem (MAGHP) respectively [e.g. Andreatta and Brunetta, 1998, Andreatta and Tidona, 1994, Estes and Ball, 2020, Mukherjee and Hansen, 2007, Richetta and Odoni, 1993, Vranas et al., 1994]. In the deterministic SAGHP and MAGHP, the airport capacity (or capacities) is assumed to be known with certainty [e.g. Andreatta and Brunetta, 1998, Andreatta and Tidona, 1994, Vranas et al., 1994]. However, in practice, airport capacity is often uncertain and can vary significantly over time. Recognizing the role that uncertainty plays in designing realistic ground holding policies, stochastic versions of the SAGHP and MAGHP (s-SAGHP and s-MAGHP, respectively) have also been examined: techniques such as stochastic programming [Corolli et al., 2017, Estes and Ball, 2020, Mukherjee and Hansen, 2005, 2007] and chance-constrained programming [Chen and Sun, 2018] have been used to model uncertainty in airport capacities. The results of these models demonstrate that stochastic formulations can balance robustness and cost, and often reduce airborne costs relative to deterministic policies.

Despite these advances, a key practical vulnerability remains: stochastic GHPs rely on a probabilistic model of future airport capacities, typically derived from weather forecasts, runway configuration predictions, and historical data. Forecast uncertainty, model estimation error, incomplete information available in operational decision support systems, and climate-driven nonstationarity can all lead to *distribution shift*, i.e., realized capacity trajectories that deviate systematically from the assumed scenario probabilities [Choi and Jin Kim, 2021, Kicing et al., 2016, Ziming et al., 2022]. When the assumed distribution is misspecified, a policy optimized for the nominal distribution can perform poorly out of sample, especially under rare but operationally consequential capacity shortfalls. This motivates an *uncertainty-of-uncertainties* perspective: even the estimated capacity distribution is itself uncertain and may change over time, so robust decision support should hedge not only against capacity realizations but also against errors in the distributional inputs.

The goal of this paper is to address these uncertainty-of-uncertainties challenges by formulating and solving a stochastic GHP that is *distributionally robust* to inaccuracies in the probabilistic airport capacity scenarios. Specifically, we propose a *distributionally robust optimization (DRO)* approach that protects against plausible distributional perturbations around an empirical capacity distribution, thereby producing ground holding policies with improved reliability under distribution shift.

1.1 Contributions

This paper makes the following contributions:

- **Distributionally robust SAGHP formulation.** We develop a distributionally robust formulation of the single-airport ground holding problem that explicitly hedges against misspecification in airport capacity distributions, addressing the practical reality that scenario probabilities derived from forecasts and historical data can be inaccurate or nonstationary.
- **A general, efficient decomposition algorithm.** We develop an efficient solution algorithm that combines Kelly’s cutting plane method with the integer L-shaped method, and that applies to a broad class of *two-stage distributionally robust integer programs* with *relatively complete recourse* and *continuous second-stage decision variables*. This method includes a novel dual bisection and primal recovery approach that leverages the structure of the distributionally robust problem to quickly generate cutting planes required by Kelly’s cutting plane method. This yields

a practical computational framework for solving the proposed distributionally robust SAGHP and, more generally, DRO models within this structural class.

- **Empirical evaluation under distribution shift.** Through numerical experiments, we assess out-of-sample performance under misspecified capacity distributions and demonstrate when distributional robustness yields substantial gains relative to deterministic and conventional stochastic SAGHP policies.

In section 2 we provide a literature review. In section 3 we define variants of the SAGHP, including dr-SAGHP, and present a deterministic equivalent for the d-SAGHP. Our proposed solution approach is given in section 4. We then conduct numerical experiments to evaluate the out-of-sample performance of the proposed distributionally robust ground holding policies against those derived from s-SAGHP in section 5.

2 Literature Review

As discussed in the introduction, our work builds on the literature on the stochastic SAGHP. While several variants of this problem and their properties have been studied in the literature [Ball et al., 2003, Chen and Sun, 2018, Estes and Ball, 2020, Glover and Ball, 2013, Mukherjee and Hansen, 2005, 2007, e.g.], we are the first to solve the distributionally robust variant. As we will show, this provides better performance in the presence of distributional drift or misspecification.

2.1 Stochastic Air Traffic Flow Management

More broadly, there exists work on other air traffic flow management (ATFM) problems under uncertainty beyond GHPs. For example, [Agustí et al., 2012, Corolli et al., 2017] provide two-stage and multistage stochastic integer programs respectively for problems in which tactical decisions, such as ground delay, airborne holding, and flight rerouting, are optimized against sampled capacity scenarios. Chance-constrained formulations have also been used to control the risk of capacity violations under disruptive weather by bounding the probability that sector capacities are exceeded [Chen et al., 2017]. In addition, a robust and adaptive approach has been proposed for ATFM under weather-driven capacity uncertainty [Gupta and Bertsimas, 2011]. In comparison to approach, the approach [Gupta and Bertsimas, 2011] is pointwise robust rather than distributionally robust. That is, our approach minimizes worst-case expected value across a collection of distributions, while the approach [Gupta and Bertsimas, 2011] minimizes the worst-case realized value across a collection of realizations. The pointwise approach to robustness tends to be much more conservative in terms of the solutions produced, which causes the solutions to have lower expected performance. Collectively, this literature demonstrates the value of explicitly modeling capacity uncertainty, while also highlighting the sensitivity of solutions to scenario generation and the assumed probabilistic description of the underlying weather and capacity processes. The same benefits that distributionally robust optimization provide for GHPs in the face of climate change may also apply to other types of (ATFM) problems. We leave this as an avenue of future research.

2.2 Distributionally Robust Optimization

Distributionally robust optimization (DRO) provides a complementary approach for decision-making under uncertainty when the true probability law is not known with confidence. Rather than optimizing the expected value with respect to a single estimated distribution, DRO optimizes the worst-case expected value amongst a family of plausible distributions, referred to as an *ambiguity set*, constructed around empirical evidence and modeling assumptions [Delage and Ye, 2010, Esfahani and Peyman, 2018, Ruiwei et al., 2019, Zhen et al., 2021]. Prior work has proposed ambiguity sets based on distributional moments and on statistical distances, with distance-based constructions (including Wasserstein-based sets) receiving particular attention due to their favorable out-of-sample performance and tractable reformulations in many settings [Esfahani and Peyman, 2018, Zhen et al., 2021]. In this paper, we adopt a Wasserstein-type ambiguity set for airport capacity uncertainty and develop distributionally robust formulations of both the single-airport and multi-airport ground holding problems. This allows the resulting ground holding policies to hedge against errors in the scenario probabilities

and against distributional shifts that arise from upstream forecast uncertainty and changing weather regimes.

2.3 Climate Change Impacts

A growing body of attribution and process-based evidence indicates that anthropogenic climate change is already altering the frequency and intensity characteristics of several high-impact weather hazards. Event-attribution syntheses find especially robust signals for increased likelihood and/or intensity of heat extremes and heavy rainfall, with more mixed or regionally dependent signals for drought and some storm types [Clarke et al., 2022, Faranda et al., 2022]. For tropical cyclones, recent work links observed global increases in rapid intensification to thermodynamic environments that have become more favorable under anthropogenic warming, increasing the probability of conditions conducive to very fast storm strengthening [Bhatia et al., 2022]. In the hydrologic domain, a central implication is the breakdown of stationarity assumptions used in risk analysis and design: climate-driven non-stationarity and deep uncertainty imply that return levels and return periods of floods and extreme precipitation should be treated as time-varying quantities rather than fixed constants [Mondal and Mujumdar, 2016]. Empirically and in downscaled projections, multiple studies show that short-duration rainfall extremes are intensifying and that standard intensity–duration–frequency (IDF) relationships can shift materially over time, motivating periodic updating of design curves and climate-informed frequency estimation for resilient infrastructure planning [Doulabian et al., 2023, Maity and Maity, 2022, Nagai and Bormudoi, 2026, Tamm et al., 2023]. Together, these findings support a planning paradigm in which weather extremes are both intensifying and becoming less well-described by historical distributions, increasing the value of decision methods that remain robust under distributional change and imperfect probabilistic information.

Climate change affects transportation systems through both gradual shifts in baseline conditions and changes in extreme-event regimes that drive disruptions, damages, and cascading failures across interdependent networks. Reviews of road transport infrastructure document multiple climate-sensitive failure and degradation pathways—including flooding and scour, coastal inundation and sea-level rise impacts on low-lying assets, landslides, and heat-related deterioration of pavements and structures—and emphasize that effective adaptation typically combines engineering hardening, improved drainage and design standards, operational measures, and risk-informed asset management [de Abreu et al., 2022, Moretti and Loprencipe, 2018]. The resilience literature further highlights that transportation performance impacts are system-level: weather shocks propagate via network connectivity, capacity reductions, and recovery constraints, so evaluating resilience requires moving beyond static risk notions toward robustness, redundancy, rapidity of recovery, and adaptive capacity [Jaroszweski et al., 2014, Markolf et al., 2019, Zhou et al., 2019].

3 The Distributional Robust Single Airport Ground Holding Problem

Distributionally Robust Optimization is a variation of stochastic optimization techniques that can handle distributional uncertainties by defining an ambiguity set that represents a set of possible distributions for stochastic input parameters. In this section, we present the deterministic SAGHP Andreatta and Brunetta [1998], define stochastic and distributionally robust variants of the SAGHP, and derive a deterministic equivalent form of the distributionally robust SAGHP under the Wasserstein ambiguity set. In aviation specifically, adaptation-focused synthesis shows that climate change can influence operations and capacity through changes in temperature, precipitation, sea-level rise, winds, and more extreme weather (e.g., convective activity), with consequences for airports and air traffic management including weather-driven capacity shortfalls, schedule disruption, and the need for proactive adaptation planning and decision support [Ryley et al., 2020]. Overall, these studies converge on the idea that climate change is increasing both the magnitude of weather-driven disruptions and the uncertainty surrounding when/where they occur, implying that transportation planning and operations benefit from models that explicitly account for non-stationary hazards and robustness to probabilistic misspecification.

3.1 Deterministic and Two-Stage Stochastic formulations of SAGHP

We begin by presenting a deterministic model for the SAGHP, which we refer to as d-SAGHP. d-SAGHP is a special case of a multi-airport model proposed in Vranas et al. [1994] and referred to as the VBO model in Andreatta and Brunetta [1998]. A fundamental assumption of this model is that airport congestion arises solely from insufficient arrival capacity, while departure capacity is assumed to be infinite and does not impose a bottleneck on operations. While we focus on the single airport case, similar methods could be applied to the multi-airport case.

The objective of d-SAGHP is to minimize total ground holding delay by strategically shifting delays from the airborne phase to the ground phase. The operational environment is governed by three categories of constraints:

1. **Capacity constraints (1b):** Bound the number of arrivals within a given time period based on airport capacity;
2. **Assignment constraints (1c):** Ensure each flight f is assigned a unique actual arrival time $t \in T_f$
3. **Coupling constraints (1d):** Preserve the temporal dependencies between preceding and successive connecting flights $(f_1, f_2) \in \mathcal{C}$ based on the buffer S_{f_1, f_2}

Table 1. Sets, Parameters, and Decision Variables

Notation	Description
<i>Sets and Indices</i>	
T	Set of time periods, indexed by t
F	Set of flights destined for the impacted airport, indexed by f
\mathcal{C}	Set of connecting flight pairs (f_1, f_2)
T_f	Set of available actual arrival times for flight f , $T_f = \{r_f, \dots, T\}$
Ξ	Set of scenarios of underlying uncertainty, indexed by ξ
<i>Parameters</i>	
r_f	Scheduled arrival time of flight f
C_g	Unit ground holding cost
C_h	Unit airborne holding cost
S_{f_1, f_2}	Maximum delay for f_1 without affecting successive flight f_2
\hat{P}	estimated distribution on Ξ
<i>Decision Variables</i>	
$x_{f,t}$	Binary variable; 1 if flight f lands at time t , 0 otherwise
$y_t(\xi)$	Number of holding flights at time t in scenario ξ

The mathematical formulation of d-SAGHP is shown as follow:

$$\min_x \sum_{f \in F} C_g \left(\sum_{t \in T_f} t x_{f,t} - r_f \right) \quad (1a)$$

$$\text{s.t.} \quad \sum_{f \in F} x_{f,t} \leq K, \forall t \in T, \quad (1b)$$

$$\sum_{t \in T_f} x_{f,t} = 1, \forall f \in F, \quad (1c)$$

$$\begin{aligned} & \sum_{t \in T_{f_1}} t x_{f_1,t} - r_{f_1} + S_{f_1, f_2} \\ & \leq \sum_{t \in T_{f_2}} t x_{f_2,t} - r_{f_2}, \forall (f_1, f_2) \in \mathcal{C}, \end{aligned} \quad (1d)$$

$$x_{f,t} \in \{0, 1\}, \forall f \in F, \forall t \in T_f. \quad (1e)$$

We next present a two-stage stochastic variant of the SAGHP, which we refer to as s-SAGHP. In the s-SAGHP, the capacity of the impacted airport to accommodate arriving aircraft is uncertain. The central modeling assumption of the s-SAGHP is that departure times of flights are chosen at the beginning of the planning horizon, before airport capacity is revealed. It is then possible that the number of flights attempting to land in some time period is in excess of capacity. In such a case, it is necessary for some flights to be held in the air until the next time period. The goal is to minimize an expected total cost of ground and air holding.

Let Ξ represent a set of possible scenarios or realizations of the uncertain elements that affect the problem. We then model the airport capacity as a T -dimensional random variable K , with $K_t(\xi)$ giving the number of flights that may arrive at the airport in time period t under scenario ξ . The s-SAGHP requires some estimated distribution \hat{P} on Ξ . Often, the empirical distribution is used based on some historical data. Then, s-SAGHP is given as follows:

$$\min_x \left\{ \sum_{f \in F} C_f \left(\sum_{t \in T_f} t x_{f,t} - r_f \right) + \mathbb{E}_{\xi \sim \hat{P}} [Q(x, \xi)] \right\} \quad (2a)$$

s.t. (1c),(1d) and (1e).

where the recourse $Q(x, \xi)$ is formulated as:

$$Q(x, \xi) := \min \sum_{t=0}^{T_{\max}} C_h y_t(\xi) \quad (3a)$$

s.t.

$$y_t(\xi) \geq y_{t-1}(\xi) + \sum_{f \in F} x_{f,t} - K_t(\xi) \quad (3b)$$

$$\forall t = 1, \dots, T_{\max},$$

$$y_0(\xi) \geq \sum_{f \in F} x_{f,0} - K_0(\xi), \quad (3c)$$

$$y_t(\xi) \geq 0, \quad \forall t = 0, \dots, T_{\max}. \quad (3d)$$

The objective function (2a) is the sum of ground holding delays for all flights and the expected air delays in the second stage. The first stage constraints of d-SAGHP consist of the same constraints in s-SAGHP except for the airport capacity constraints, which are imposed in the second stage. The second stage decision variable $y_t(\xi)$ represents the number of arrival flights joining the arrival queue or conducting airborne holding around the terminal area in scenario ξ . The second stage objective (3a) is to minimize the airborne delay cost. As for the constraints of the second stage problem, (3b) is the second stage capacity constraint. Intuitively, the expression $y_{t-1}(\xi) + \sum_{f \in F} x_{f,t}$ gives the number of flights in the terminal airspace at time t . At most $K_t(\xi)$ such flights will be able to land, and any remaining flights must be held to the next time period. Constraint (3c) is second stage capacity constraint at time period 0. This constraint follows a similar format as constraint (3b), with the assumption that no flights are held in the air prior to the initiation of the planning horizon. The magnitude of the unit cost of airborne delays is typically greater than that for ground delays.

3.2 Wasserstein Ambiguity Set for Discrete Measures

We assume that airport capacity distributions are discrete probability distributions, which is typically true of airport capacity data. Therefore, we assume Ξ is finite and we restrict our discussion to Wasserstein ambiguity sets for discrete distributions. We note that in practice, while the set of possible capacity distributions is finite, it may be prohibitively large. There are several possible strategies for overcoming this obstacle. In this paper, we treat the support of the empirical distribution as if it were the entire support of the distribution for the purposes of formulating and solving the ground holding problem. Even though this may omit some elements of the true support, we found that this

approach still provide solutions that were significantly more robust than the s-SAGHP with respect to uncertainty drawn from the entire sample space; see Section 5.

Let $\{\xi_1, \dots, \xi_{|\Xi|}\}$ denote the elements of Ξ . Each probability measure on Ξ can be represented as a $|\Xi|$ -dimensional vector p where p_i gives the probability of scenario ξ_i .

Given distributions q and p in $\mathbb{R}^{|\Xi|}$, we let $\mathcal{D}(q, p)$ denote the set of $n \times n$ matrices $(\pi_{i,j})_{i \leq n; j \leq n}$ in $[0, 1]^{n \times n}$ satisfying the marginal constraints: $\sum_{i=1}^n \pi_{i,j} = q_i$ and $\sum_{i=1}^n \pi_{i,j} = p_j, \forall i = 1, \dots, n; j = 1, \dots, n$. Let $d_{i,j}$ denote the distance between scenario ξ_i and ξ_j under some distance measure. Then the Wasserstein distance for two discrete measures q and p is defined to be:

$$W(q, p) = \inf_{\pi \in \mathcal{D}(q, p)} \sum_{i,j} \pi_{i,j} d_{i,j} \quad (4)$$

The Wasserstein ambiguity set centered around an estimated distribution \hat{p} with radius $\varepsilon \geq 0$, denoted as $\mathcal{P}_\varepsilon(\hat{p})$, is then given by

$$\mathcal{P}_\varepsilon(\hat{p}) := \left\{ q \in \mathbb{R}^{|\Xi|} : W(p, q) \leq \varepsilon \right\}. \quad (5)$$

The dr-SAGHP is similar to the s-SAGHP. However, rather than minimizing the expected ground and air holding cost with respect to estimated distribution \hat{P} , the dr-SAGHP minimizes the worst case expected costs amongst the distributions in a Wasserstein ball centered at \hat{P} . This is formulated as follows:

$$\begin{aligned} \min_x & \left\{ \sum_{f \in F} C_f \left(\sum_{t \in T_f} t x_{f,t} - r_f \right) + \right. \\ & \left. \max_{p \in \mathcal{P}_\varepsilon(\hat{P})} \mathbb{E}_p [Q(x, \xi)] \right\} \\ \text{s.t.} & \quad (1c) - (1e). \end{aligned} \quad (6)$$

The dr-SAGHP is often solved by producing a deterministic equivalent formulation, such as that proposed in Esfahani and Peyman [2018]. We have produced such a deterministic equivalent:

$$\min_{x, \lambda, \alpha} \left\{ \sum_{f \in F} C_f \left(\sum_{t \in T_f} t x_{f,t} - r_f \right) + \lambda \varepsilon + \sum_{i=1}^n \alpha_i \hat{p}_i \right\} \quad (7a)$$

$$\begin{aligned} \text{s.t.} \quad \alpha_i + \lambda d_{i,j} & \geq \sum_{t \in T} C_h y_t(\xi_j), \\ & \forall i, j \in \{1, \dots, |\Xi|\}, \end{aligned} \quad (7b)$$

$$\begin{aligned} y_t(\xi) - y_{t-1}(\xi) & \geq \sum_{f \in F} x_{f,t} - K_t(\xi), \\ & \forall t \in T, \xi \in \Xi, \end{aligned} \quad (7c)$$

$$y_0(\xi) \geq \sum_{f \in F} x_{f,0} - K_0(\xi), \quad \forall \xi \in \Xi, \quad (7d)$$

$$\sum_{t \in T_f} x_{f,t} = 1, \quad \forall f \in F, \quad (7e)$$

$$\begin{aligned} & \sum_{t \in T_{f_2}} t x_{f_2,t} - r_{f_2} \\ & \geq \sum_{t \in T_{f_1}} t x_{f_1,t} - r_{f_1} - S_{f_1, f_2}, \quad f_1, f_2 \in \mathcal{C}, \end{aligned} \quad (7f)$$

$$y_t(\xi) \geq 0, \quad \forall f \in F, t \in T, \xi \in \Xi, \quad (7g)$$

$$x_{f,t} \in \{0, 1\}, \forall f \in F, t \in T \quad (7h)$$

$$\lambda \geq 0 \quad (7i)$$

The derivation is given in Appendix A.

4 Decomposition Approach

In the deterministic equivalent formulation of problem (28), the number of distributionally robust constraints (28b) grows quadratically with the number of scenarios in the support set $\widehat{\Xi}$. This rapid growth in constraints significantly increases computational complexity for a large number of scenarios. To address this issue and provide a more scalable solution method, we develop a decomposition approach that avoids the explicit enumeration of all distributionally robust constraints and makes the solution process more efficient.

4.1 Preliminaries

We begin by introducing a general two-stage distributionally robust mixed-integer linear program

$$\begin{aligned} \min_{\mathbf{x}} \quad & \mathbf{c}^\top \mathbf{x} + \max_{p \in \mathcal{P}_\varepsilon(\widehat{P})} \mathbb{E}_p[h(\mathbf{x}, \xi)] \\ \text{s.t.} \quad & \mathbf{A}\mathbf{x} = \mathbf{b} \\ & \mathbf{x} \in \{0, 1\}^N \end{aligned} \tag{8}$$

where \mathbf{c} is an N -dimensional vector, \mathbf{A} is an $M \times N$ matrix, \mathbf{b} is an M -dimensional vector, and h is a recourse function $h: \mathbb{R}^N \times \Xi \rightarrow \mathbb{R}$. The assumption that \mathbf{x} is a vector of pure binary variables is made solely for convenience; a similar approach applies to general integer or mixed variables.

As in previous sections, we assume that the set of possible scenarios Ξ is finite. This assumption is not routinely made in distributionally robust settings, but is applicable to many real-world settings. This includes air traffic flow management settings, where the capacity is often discrete.

In addition, we define

$$f(\mathbf{x}) = \max_{p \in \mathcal{P}_\varepsilon(\widehat{P})} \mathbb{E}_{\xi \sim p}[h(\mathbf{x}, \xi)]$$

and assume that $h(\cdot, \xi)$ is convex, which implies that f will likewise be convex; for each fixed distribution $p \in \mathcal{P}_\varepsilon(\widehat{P})$ the function $\mathbf{x} \mapsto \mathbb{E}_p[h(\mathbf{x}, \xi_i)] = \sum_{i=1}^{|\Xi|} p_i h(\mathbf{x}, \xi_i)$ is convex, as it is sum of convex functions multiplied by non-negative values, and taking the maximum of a collection of convex functions preserves convexity. The recourse $h(\cdot, \xi)$ is typically true when the second stage is the objective value of a linear program, as in the dr-SAGHP. However, this is not typically true when the second stage contains some integer variables, in which case adjustments may be required to our approach. We leave such an extension as an avenue of future work.

Finally, we assume that $\mathbb{E}_p[h(\mathbf{x}, \xi)]$ is finite for each $p \in \mathcal{P}_\varepsilon(\widehat{P})$ and for each $\mathbf{x} \in \{0, 1\}^N$ satisfying $\mathbf{A}\mathbf{x} = \mathbf{b}$. This is similar to the assumption of relatively complete recourse, often made in stochastic programming (see, e.g. chapter 5 of Birge and Louveaux [1997]). In the case that the second stage is the objective value of a linear program, our method could be readily extended to the case where relatively complete recourse does not apply through the addition of standard Benders' feasibility cuts (e.g., section 6.5 of Bertsimas and Tsitsiklis 1997).

4.2 Cutting plane approach

We first develop a decomposition algorithm to solve the linear programming relaxation of Problem (8). Our approach is a specialization of Kelly's cutting plane algorithm [Kelley, 1960] that leverages the structure of the distributionally robust optimization problem to efficiently produce cuts. Such a constant can be shown to exist since f is convex. We recast the LP relaxation of formulation (8) in its epigraph form:

$$\min_{\mathbf{x}} \quad \mathbf{c}^\top \mathbf{x} + \theta \tag{9a}$$

$$\text{s.t.} \quad \mathbf{A}\mathbf{x} = \mathbf{b} \tag{9b}$$

$$\theta \geq f(\mathbf{x}), \tag{9c}$$

$$\mathbf{x} \in [0, 1]^N \tag{9d}$$

Let L be a constant such that $f(\mathbf{x}) \geq L$ for all $x \in [0, 1]^N$, which must exist due to the convexity of f . Since f is convex, then, as in Kelley [1960], we can approximate the constraints (9c) with a collection of constraints of the form:

$$\begin{aligned} \theta &\geq L \\ \theta &\geq f(\mathbf{x}^k) + (s^k)^\top(\mathbf{x} - \mathbf{x}^k) \text{ for } i \in \{1, \dots, K\} \end{aligned} \tag{10}$$

where $\{\mathbf{x}^1, \dots, \mathbf{x}^K\}$ are a collection of feasible test points, and where each vector s^k is a corresponding subgradient of f at \mathbf{x}^k . The points $\mathbf{x}^1, \dots, \mathbf{x}^K$ are generated iteratively. In particular, once K points have been generated, the point x^{K+1} is the optimal solution to the problem produced by the first K cuts. Replacing constraints (9c) with the approximation (10) produces a relaxation of the problem. Thus, if we let \hat{z}^K be the optimal objective value of the relaxation with K cuts added and we let z^* be the optimal objective value of problem (8), we have that $\hat{z}^K \leq z^*$. Furthermore, since \mathbf{x}^K is feasible, the objective value $f(\mathbf{x}^K) \geq z^*$. Thus, in each iteration, the difference $f(\mathbf{x}^K) - \hat{z}^K$ provides an optimality gap, and the algorithm may be terminated once this gap is sufficiently small. See Algorithm 1. For any fixed optimality gap, the algorithm converges within a finite number of iterations [Kelley, 1960].

Algorithm 1 Kelly's cutting plane algorithm.

Input: tolerated optimality gap η .
for $K = 1, 2, \dots$ **do**
 Solve:
 $\min_{\mathbf{x}} \mathbf{c}^\top \mathbf{x} + \theta$
 s.t. $\mathbf{A}\mathbf{x} = \mathbf{b}$
 $\theta \geq L$
 $\theta \geq f(\mathbf{x}^k) + (s^k)^\top(\mathbf{x} - \mathbf{x}^k) \forall k \in \{1, \dots, K-1\}$
 $\mathbf{x} \in [0, 1]^N$
 Let \mathbf{x}^K be the solution and \hat{z}^K be the optimal value.
 if $f(\mathbf{x}^K) - \hat{z}^K \leq \eta$ **then**
 return \mathbf{x}^*
 end if
 Calculate a subgradient $s^K \in \partial f(\mathbf{x}^K)$
end for

Our method leverages the structure of the function f arising from the distributionally robust setting in order to efficiently calculate the subgradients. We apply Danskin's Theorem to relate the subdifferential of f to the subdifferentials of the recourse function in the scenarios. Given a feasible first-stage solution \mathbf{x} , let $\mathcal{P}_\varepsilon^*(\mathbf{x})$ be the set of maximizers of $\max_{p \in \mathcal{P}_\varepsilon} \mathbb{E}[h(\mathbf{x}, \varepsilon)]$.

Proposition 4.1. *Let x be any point in \mathbb{R}^n such that $\mathbf{A}\mathbf{x} = \mathbf{b}$ and $\mathbf{x} \geq 0$. Then,*

$$\partial f(\mathbf{x}) = \left\{ \sum_{i=1}^{|\Xi|} p_i^* s^i : p^* \in \mathcal{P}_\varepsilon^*(\mathbf{x}), s^i \in \partial_{\mathbf{x}} h(\mathbf{x}, \xi_i) \right\}$$

where $\partial_{\mathbf{x}} h(\mathbf{x}, \xi)$ denotes the subdifferential of $h(\cdot, \xi)$ at \mathbf{x} .

A proof of Proposition 4.1 is given in Appendix B. In essence, Proposition 4.1 states that calculating a subgradient in $\partial f(\mathbf{x})$ can be accomplished by calculating the corresponding worst-case distribution $p^*(\mathbf{x})$, calculating a subgradient of the recourse function in $\partial_{\mathbf{x}} h(\mathbf{x}, \xi_i)$ for each scenario, and then combining the two.

We assume that a subgradient in $\partial_{\mathbf{x}} h(\mathbf{x}, \xi_i)$ can be computed without excessive computational effort. In cases such as the dr-SAGHP wherein the recourse function $h(\mathbf{x}, \xi_i)$ is the objective value of a second stage linear program, it follows from standard results in stochastic programming that the subgradient can be calculated from the dual optimal variables of the second stage (see, for example, chapter 2 of Shapiro et al. 2021). In particular, for the dr-SAGHP, the dual of the second stage given

first stage action \mathbf{x} and scenario ξ is given by:

$$\max_{\nu(\xi) \in \mathbb{R}^{T_{\max}}} \sum_{t=0}^{T_{\max}} \left(\sum_{f \in F} x_{f,t} - K_t(\xi) \right) \nu_t(\xi) \quad (11)$$

$$\text{s.t. } \nu_0(\xi) - \nu_1(\xi) \leq C_h, \quad (12)$$

$$\nu_t(\xi) - \nu_{t+1}(\xi) \leq C_h, \quad (13)$$

$$\forall t = 1, \dots, T_{\max} - 1,$$

$$\nu_{T_{\max}}(\xi) \leq C_h, \quad (14)$$

$$\nu_t(\xi) \geq 0, \quad \forall t = 0, \dots, T_{\max}. \quad (15)$$

Then, if we let $\nu^*(\mathbf{x}, \xi)$ denote an optimal solution, a subgradient $s(\xi)$ of the recourse function $Q(\cdot, \xi)$ at \mathbf{x} is given by letting $s_{f,t}(\xi) = \nu_t^*(\xi)$ for all $f \in F$ and $t \in \{0, \dots, T_{\max}\}$. Then, if we can identify a distribution $p_i^*(\mathbf{x}) \in \mathcal{P}_\varepsilon^*(\mathbf{x})$, the cut that is generated at the test point \mathbf{x}^k is given by:

$$\begin{aligned} \theta &\geq \sum_{i=1}^{|\Xi|} p_i^*(\mathbf{x}^k) Q(\mathbf{x}^k, \xi_i) \\ &+ \sum_{i=1}^{|\Xi|} p_i^*(\mathbf{x}^k) \sum_{t=0}^{T_{\max}} \nu_t^*(\mathbf{x}^k, \xi_i) \left(\sum_{f \in F} x_{f,t} - x_{f,t}^k \right) \end{aligned}$$

By strong duality, $Q(x^k, \xi_i) = \sum_{t=0}^{T_{\max}} \nu_t^*(\mathbf{x}^k, \xi_i) \left(\sum_{f \in F} x_{f,t}^k - K_t(\xi_i) \right)$, so this can be simplified to:

$$\theta \geq \sum_{i=1}^{|\Xi|} p_i^*(\mathbf{x}) \sum_{t=0}^{T_{\max}} \nu_t^*(\mathbf{x}, \xi_i) \left(\sum_{f \in F} x_{f,t} - K_t(\xi_i) \right),$$

4.3 Calculating the worst-case distribution

Using the fact that the set Ξ is discrete, we provide an efficient method for calculating the inner maximization problem $\max_{p \in \mathcal{P}_\varepsilon} \mathbb{E}_{\xi \sim p} [h(\mathbf{x}, \xi)]$ for a fixed, feasible first stage decision \mathbf{x} . Throughout this section, we treat the first stage decision \mathbf{x} as fixed. It follows from the definition of the Wasserstein ambiguity set that this problem can be formulated as follows:

$$\max_{\pi \in [0,1]^{|\Xi|} \times |\Xi|} \sum_{i=1}^{|\Xi|} \sum_{j=1}^{|\Xi|} \pi_{i,j} h(\mathbf{x}, \xi_j) \quad (16a)$$

$$\text{s.t. } \sum_{i=1}^{|\Xi|} \sum_{j=1}^{|\Xi|} \pi_{i,j} d_{i,j} \leq \varepsilon \quad (16b)$$

$$\sum_{j=1}^{|\Xi|} \pi_{i,j} = \hat{p}_i, \quad \forall i \quad (16c)$$

$$\pi_{i,j} \geq 0, \quad \forall i, j \quad (16d)$$

Given a solution π^* , the corresponding optimal distribution is given by $p_j^* = \sum_{i=1}^{|\Xi|} \pi_{i,j}^*$ for each $j \in \{1, \dots, |\Xi|\}$. The dual of problem (16) follows:

$$\min_{\lambda \in \mathbb{R}, \alpha \in \mathbb{R}^{|\Xi|}} \lambda \varepsilon + \sum_{i=1}^{|\Xi|} \alpha_i \hat{p}_i \quad (17a)$$

$$\text{s.t. } \alpha_i + \lambda d_{i,j} \geq h(\mathbf{x}, \xi_j), \quad \forall i, j, \quad (17b)$$

$$\lambda \geq 0. \quad (17c)$$

We can reduce the dual problem (17) to a univariate optimization problem. First, note that for any $\lambda \geq 0$, there exists $\alpha \in \mathbb{R}^{|\Xi|}$ such that (λ, α) is feasible for (16). In particular, if we let each α_i be

any value no smaller than $\max_{j \in \{1, \dots, |\Xi|\}} (h(\mathbf{x}, \xi_j) - \lambda d_{i,j})$, then (λ, α) is feasible. Furthermore, since the coefficient of α_i is given by \widehat{p}_i , which is non-negative, the optimal choice of α_i given fixed λ is given by $\alpha_i^*(\lambda) := \max_{j \in \{1, \dots, |\Xi|\}} (h(\mathbf{x}, \xi_j) - \lambda d_{i,j})$. Thus, the problem reduces to that of minimizing the function $\phi : \mathbb{R} \rightarrow \mathbb{R}$ given by:

$$\begin{aligned} \phi(\lambda) &:= \lambda \varepsilon + \sum_{i=1}^{|\Xi|} \alpha_i^*(\lambda) \widehat{p}_i \\ &= \lambda \varepsilon + \sum_{i=1}^{|\Xi|} \widehat{p}_i \max_{j \in \{1, \dots, |\Xi|\}} (h(\mathbf{x}, \xi_j) - \lambda d_{i,j}). \end{aligned} \quad (18)$$

Proposition 4.2. *Let λ^* be a solution to $\min_{\lambda \geq 0} \phi(\lambda)$. Then $(\lambda^*, \alpha^*(\lambda^*))$ is an optimal solution to problem (17)*

The function ϕ is piecewise-linear convex, as each function $\lambda \mapsto \max_{j \in \{1, \dots, |\Xi|\}} (h(\mathbf{x}, \xi_j) - \lambda d_{i,j})$ is a piecewise-linear convex function and each $\widehat{p}_i \geq 0$. A proof of Proposition 4.2 is given in Appendix C.

We therefore develop a bisection scheme, given in Algorithm 2, to compute the optimal dual multiplier λ^* . The algorithm requires as a starting point lower and upper bounds λ_{lo} and λ_{hi} such that there exists a minimizer λ^* in the interval $[\lambda_{\text{lo}}, \lambda_{\text{hi}}]$. The algorithm also requires a prespecified tolerance δ , and produces an solution that is within δ of an optimal solution.

At each iteration, Algorithm 2 chooses a test point $\lambda = (\lambda_{\text{hi}} + \lambda_{\text{lo}})/2$ at the middle of the interval and evaluates a subgradient $\partial\phi(\lambda)$. If the subgradient is positive, this implies that there exists an optimal value λ^* such that $\lambda^* \leq \lambda$, whence we can update the upper bound λ_{hi} to λ . Similarly, if the subgradient is negative, the lower bound λ_{lo} may be updated to λ . If the subgradient is identically zero, then λ is optimal. This continues until the lower bound and upper bound within the specified tolerance, or an optimal solution is found.

Proposition 4.3. *Algorithm 2 stops after at most $\lceil \log_2(\frac{\lambda_{\text{hi}} - \lambda_{\text{lo}}}{\delta}) \rceil$ iterations and returns a value λ such that $(\lambda - \delta, \lambda + \delta) \cap \arg \min_{\lambda \geq 0} \phi(\lambda)$ is non-empty. Here, λ_{hi} and λ_{lo} refer to the initial values of these variables input into Algorithm 2.*

A proof of Proposition 4.3 is given in Appendix D. In order to implement Algorithm 2, we must identify the initial valid lower bounds and upper bounds. By definition, 0 is a valid lower bound; we can provide a valid upper bound that can be readily computed.

Algorithm 2 Dual Bisection Algorithm

- 1: Inputs: first stage feasible solution $\mathbf{x} \in [0, 1]^N$; tolerance $\delta > 0$; values λ_{lo} and λ_{hi} such that $[\lambda_{\text{lo}}, \lambda_{\text{hi}}] \cap \arg \min_{\lambda \geq 0} \phi(\lambda)$ is non-empty.
 - 2: **while** $\lambda_{\text{hi}} - \lambda_{\text{lo}} > 2\delta$ **do**
 - 3: $\lambda \leftarrow \frac{1}{2}(\lambda_{\text{lo}} + \lambda_{\text{hi}})$
 - 4: For each $i \in \{1, \dots, |\Xi|\}$, choose $j^*(i, \lambda) \in \arg \min\{h(\mathbf{x}, \xi_j) - \lambda d_{i,j}\}$
 - 5: **if** $\varepsilon - \sum_{i=1}^{|\Xi|} p_i d_{ij^*(i, \lambda)} > 0$ **then**
 - 6: $\lambda_{\text{hi}} \leftarrow \lambda$
 - 7: **else if** $\varepsilon - \sum_{i=1}^{|\Xi|} p_i d_{ij^*(i, \lambda)} < 0$ **then**
 - 8: $\lambda_{\text{lo}} \leftarrow \lambda$
 - 9: **else**
 - 10: Return λ
 - 11: **end if**
 - 12: **end while**
 - 13: $\lambda^* \leftarrow \frac{1}{2}(\lambda_{\text{lo}} + \lambda_{\text{hi}})$
 - 14: **return** λ^*
-

Proposition 4.4. *If the Wasserstein ambiguity radius $\varepsilon > 0$, then all optimal solutions to $\min_{\lambda \geq 0} \phi(\lambda)$ are less than or equal to*

$$\frac{\max_{j \in \{1, \dots, |\Xi|\}} h(\mathbf{x}, \xi_j) - \min_{i \in \{1, \dots, |\Xi|\}} h(\mathbf{x}, \xi_i)}{\min_{i,j: d_{i,j} \neq 0} d_{i,j}}$$

While Algorithm 2 yields an optimal dual multiplier λ^* , the cutting planes applied in constraint (10) require the primal optimal solution to $\min_{p \in \mathcal{P}_\varepsilon} \mathbb{E}_{\xi \sim p}[h(\mathbf{x}, \xi)]$. For this reason, we develop a primal recovery procedure, given in Algorithm 3. Let $\hat{\pi}$ denote the transportation plan constructed by Algorithm 3 using λ^* . Intuitively, the transportation plan $\hat{\pi}$ is constructed in order to satisfy complementary slackness with the dual solution $(\lambda^*, \alpha^*(\lambda^*))$. The probability mass at some scenario ξ_i is transported only to scenarios ξ_j for which the value $h(\mathbf{x}, \xi_j) - \lambda^* d_{ij}$ is maximal; this is done to satisfy the complementary slackness condition $\hat{\pi}_{ij}(h(\mathbf{x}, \xi_j) - \lambda^* d_{ij}) = 0$. If $\lambda^* = 0$ then ties are broken by moving mass to the closest point. If $\lambda^* > 0$, then the transportation plan is carefully chosen to ensure that the resulting transportation costs are exactly ε , in order to satisfy the complementary slackness condition $\lambda^*(\varepsilon - \sum_{i=1}^{|\Xi|} \sum_{j=1}^{|\Xi|} \hat{\pi}_{ij}) = 0$. In either case, we can show that the resulting plan is feasible and satisfies complementary slackness with $(\lambda^*, \alpha^*(\lambda^*))$.

Theorem 4.1. *Let λ^* be an optimal solution to the dual problem (18). Then $\hat{\pi}$ is a primal optimal solution to (16).*

Algorithm 3 Primal recovery from an optimal dual multiplier λ^*

Input. Feasible first stage solution $\mathbf{x} \in [0, 1]^{\mathbf{N}}$, optimal dual multiplier $\lambda^* \geq 0$.

Output. A transportation plan $\hat{\pi} \in [0, 1]^{|\Xi| \times |\Xi|}$.

Step 1 For each $i \in \{1, \dots, |\Xi|\}$, define

$$A_i(\lambda^*) := \arg \max_{j \in \{1, \dots, |\Xi|\}} \{h(\mathbf{x}, \xi_j) - \lambda^* d_{ij}\}.$$

Select two representatives

$$\underline{j}(i) \in \arg \min_{j \in A_i(\lambda^*)} d_{ij}, \quad \bar{j}(i) \in \arg \max_{j \in A_i(\lambda^*)} d_{ij}.$$

Step 2 Define the lower and upper achievable transportation costs

$$\underline{\gamma} := \sum_{i=1}^n \hat{p}_i d_{i, \underline{j}(i)}, \quad \bar{\gamma} := \sum_{i=1}^n \hat{p}_i d_{i, \bar{j}(i)}.$$

Set

$$\beta := \begin{cases} \frac{\varepsilon - \underline{\gamma}}{\bar{\gamma} - \underline{\gamma}}, & \text{if } \lambda^* > 0 \text{ and } \bar{\gamma} > \underline{\gamma}, \\ 0, & \text{if } \lambda^* = 0 \text{ or } \bar{\gamma} = \underline{\gamma}. \end{cases}$$

Step 3 For each $i \in \{1, \dots, |\Xi|\}$ and $j \in \{1, \dots, |\Xi|\}$ set

$$\hat{\pi}_{ij} := \begin{cases} (1 - \beta) \hat{p}_i, & \text{if } \lambda^* > 0 \text{ and } j = \underline{j}(i), \\ \beta \hat{p}_i, & \text{if } \lambda^* > 0 \text{ and } j = \bar{j}(i), \\ \hat{p}_i, & \text{if } \lambda^* = 0 \text{ and } j = \underline{j}(i), \\ 0, & \text{otherwise.} \end{cases}$$

Algorithm 2 and Algorithm 3 together provide an approach to find a distribution $p^* \in \mathcal{P}_\varepsilon^*(\mathbf{x})$: first, Algorithm 2 is used to find an optimal dual multiplier λ^* , and second, the primal optimal solution is reconstructed using Algorithm 3. In particular, if $\hat{\pi}$ is the output of Algorithm 3, then the desired distribution p^* is given by $p_j^* = \sum_{i=1}^{|\Xi|} \hat{\pi}_{ij}$ for each $j \in \{1, \dots, |\Xi|\}$. We apply this in combination with Proposition 4.1 to quickly find subgradients of f for use in Kelly's cutting plane algorithm (Algorithm 1).

4.4 From LP Relaxation to Integer Program

The approach detailed in Section 4.2 can be incorporated into a variant of the integer L-shaped method [Laporte and Louveaux, 1993], and can be readily implemented in most branch-and-cut routines, including those used in popular commercial solvers. A tolerated optimality gap γ is specified, and at each node of the branch-and-cut procedure, Kelly’s cutting plane procedure (Algorithm 1) is used to solve the linear programming relaxation at the node with an optimality gap of η . As detailed in Section 4.3, we apply Algorithm 2 and Algorithm 3 in combination with Proposition 4.1 to efficiently calculate the subgradients required by the procedure. All cutting planes generated at each node are applied to all subsequent nodes. For the same reasons as in Laporte and Louveaux [1993], for typical branch-and-cut implementations, this converges in finite iterations to a feasible solution whose objective value is within η of the optimal solution.

5 Numerical Experiments and Discussion

In this section, we report numerical experiments that assess the performance of dr-SAGHP under distributional shifts in realized airport capacities relative to their empirical historical distributions. Our experimental setup is motivated by operational settings in which capacity degradations, potentially driven by climate change, create systematic discrepancies between predicted and realized capacity distributions. To capture temporal dependence in airport capacities, we use Gaussian Process Regression (GPR) [e.g. Williams and Rasmussen, 1995] to model the joint capacity distribution across time periods. The fitted GPR model is used solely to generate scenarios for the experimental evaluation and does not enter the problem formulation or the solution algorithm. We generate training samples from the fitted GPR model. Then, we alter the parameters the GPR parameters and generate testing samples. The alterations applied to the GPR parameters emulate different levels of climate-induced capacity degradation. This us allows us to measure the performance of the dr-SAGHP approach as compared to the s-SAGHP under distributional shifts produced by climate change. We note that, when solving the dr-SAGHP, the ambiguity set is under the assumption that the support of the capacity distribution is given by the samples in the training set. However, the testing set includes samples that were not present in the training set. Even with this simplifying assumption, as we will show in this section, the dr-SAGHP provides significant performance benefits over the s-SAGHP.

5.1 Experiment Setup

Flight schedules are obtained from the Bureau of Transportation Statistics (BTS) Bureau of Transportation Statistics [2026]. To evaluate the Ground Holding Problems (GHPs), we use the historical arrival performance at Newark Liberty International Airport (EWR) on August 1, 2023, which includes 543 flights. The airborne-to-ground delay cost ratio is set to three; that is, the unit airborne delay cost C_h is three times the unit ground delay cost C_f . For each connecting flight pair (f_1, f_2) , the minimum turnaround time S_{f_1, f_2} is fixed at three time periods (i.e., 45 minutes).

5.2 Airport Capacity Scenario Generation via Gaussian Process Regression

To construct empirical airport-capacity distributions over the planning horizon, we use historical airport capacity data from the FAA ASPM capacity dataset [Federal Aviation Administration, 2026a] and weather information from the FAA ASPM weather factors dataset [Federal Aviation Administration, 2026b]. We fit a Gaussian Process Regression (GPR) model using historical weather factors from 2021–2022. Similarly to Murça and Hansman [2018], given a testing date and the associated weather features, we use a fitted GPR model to produce a posterior distribution for the joint airport capacities over the planning horizon. In our implementation, the GPR model is trained using only weather features. Our main contribution lies not in the predictive model itself, but in explicitly incorporating the resulting uncertainty into the downstream dr-SAGHP framework. Importantly, the GPR model is used solely for scenario generation in the numerical experiments and does not affect the problem formulation or the solution algorithm.

Let $w \in \mathbb{R}^p$ denote the vector of weather factors and let $\psi(\cdot)$ map weather factors to airport

capacity. We model $\psi(\cdot)$ as a Gaussian process with mean function $m(\cdot)$ and covariance kernel $K(\cdot, \cdot)$:

$$\psi(w) \sim \mathcal{GP}(m(w), K(w, w')). \quad (19)$$

Let the training inputs (historical weather factors) and outputs (observed capacities at EWR) be denoted by \hat{w} and \hat{D} , respectively. For a given day, let the testing inputs across T time periods be $\mathbf{w} = \{w_1, \dots, w_T\}$. Under the standard GPR model with i.i.d. Gaussian observation noise of variance σ_d^2 , we have the mean and covariance of the posterior distribution as:

$$\begin{aligned} \tilde{\mu} &= \mathbb{E}[\psi(\mathbf{w}) \mid \hat{D}] = \\ & m(\mathbf{w}) + K(\mathbf{w}, \hat{w})\Sigma^{-1} \left(\hat{D} - m(\hat{w}) \right), \end{aligned} \quad (20)$$

$$\begin{aligned} \tilde{\Sigma} &= \text{Cov}[\psi(\mathbf{w}) \mid \hat{D}] = \\ & K(\mathbf{w}, \mathbf{w}) - K(\mathbf{w}, \hat{w})\Sigma^{-1}K(\hat{w}, \mathbf{w}), \end{aligned} \quad (21)$$

where $\Sigma = K(\mathbf{w}, \hat{w}) (K(\hat{w}, \hat{w}) + \sigma_d^2 I)$. Therefore, the joint capacities $\psi(\mathbf{w})$ across the T time periods follow a multivariate Gaussian distribution with the above posterior mean and covariance. We generate airport-capacity scenarios by sampling from this posterior distribution. In our experiments, we draw 1000 scenarios from the fitted GPR model and use them as samples from the nominal distribution for s-SAGHP and dr-SAGHP.

5.3 Design of sensitivity Analysis on Climate Change Impacts

To evaluate the performance of dr-SAGHP under climate-change impacts, we simulate distributional shifts in airport capacities at multiple severity levels. Specifically, we consider two channels through which climate change may affect the capacity distribution: (i) a shift in its mean and (ii) an increase in its variance. The former reflects persistent capacity degradation driven by more frequent or more severe adverse weather conditions [Bhatia et al., 2022]. The latter reflects increased uncertainty in capacity prediction due to faster-evolving and less predictable severe weather patterns [Mondal and Mujumdar, 2016].

In the sensitivity analysis, we construct the nominal (empirical) distribution using samples from the fitted GPR posterior. To generate testing distributions for mean shifts, we impose mean reductions of $r \in \{0.05, 0.10, 0.15, 0.20\}$ on the fitted GPR posterior mean and draw 1000 capacity scenarios from the resulting shifted posterior. The out-of-sample cost is evaluated by solving a stochastic program with the same structure as (2), using the ground-holding policy x^* obtained from either s-SAGHP or dr-SAGHP, and using the shifted capacity samples as input parameters.

To assess the impact of climate change on capacity variability, we increase the posterior covariance of the GPR model by scaling it as

$$\tilde{\Sigma}_\gamma = (1 + \gamma)\tilde{\Sigma}, \quad \gamma \in \{0.5, 1.0, 1.5, 2.0\},$$

so that the covariance is multiplied by factors 1.5, 2.0, 2.5, and 3.0, respectively. Larger values of γ induce greater variability in the generated capacity scenarios. For sufficiently large γ , however, some sampled capacities may exceed the physical maximum capacity of EWR. To ensure physical feasibility, we cap each sampled capacity at the airport's maximum operational capacity. When evaluating the out-of-sample performance, in addition to evaluating the expected objective value, we also evaluate performance under adverse conditions, using Conditional Value-at-Risk (CVaR). CVaR captures tail risk and thus provides information regarding of operational performance in conditions that are worse than typical. Following Rockafellar and Uryasev [2000], let $\Phi(x, \psi(\mathbf{w}))$ denote the realized cost induced by decision x under random parameters $\psi(\mathbf{w}) \sim \mathbb{P}(\psi(\mathbf{w}) \mid \hat{D})$ with a posterior density function $p_{\psi(\mathbf{w})|\hat{D}}(\cdot)$. For a confidence level $\tau \in (0, 1)$, define the value-at-risk (VaR) as

$$\begin{aligned} \zeta_\tau(x) &:= \text{VaR}_\tau(\Phi(x, \psi)) \\ &= \inf \left\{ z \in \mathbb{R} : \int_{\Phi(x, \psi) \leq z} p_{\psi|\hat{D}}(\psi) d\psi \geq \tau \right\}. \end{aligned} \quad (22)$$

Table 2. Comparison between convex reformulation and Algorithm ??.

ε	DE Obj.	K-IL Obj.	Gap (%)	DE Time (s)	K-IL Time (s)	Speed-up
0.0	2109.106	2110.436	0.063	7002.79	445.28	15.73
0.1	2552.297	2552.297	0.000	7708.21	487.65	15.81
0.2	2795.323	2795.298	0.001	7382.85	573.64	12.87
0.3	2894.856	2894.255	0.021	7415.64	477.42	15.53
0.4	2968.133	2966.319	0.061	8938.76	379.53	23.55
0.5	3022.334	3021.527	0.027	7144.85	285.08	25.06
0.6	3048.000	3046.610	0.046	20804.10	266.67	78.01
0.7	3048.000	3048.000	0.000	24145.97	245.89	98.20
0.8	3048.000	3048.000	0.000	20219.88	238.47	84.79
0.9	3048.000	3048.000	0.000	22700.69	239.73	94.69
1.0	3048.000	3048.000	0.000	24862.04	243.16	102.25

Then the corresponding conditional value-at-risk (CVaR) is

$$\begin{aligned} & \text{CVaR}_\tau(\Phi(x, \psi)) \\ &= \frac{1}{1 - \tau} \int_{\Phi(x, \psi) \geq \zeta_\tau(x)} \Phi(x, \psi) p_{\psi|\widehat{D}}(\psi) d\psi. \end{aligned} \quad (23)$$

In the sensitivity analysis, we measure the distance between any two joint capacity scenarios using a normalized ℓ_2 metric:

$$d_{i,j} = \frac{\|\widehat{\xi}_i - \widehat{\xi}_j\|_2}{\max_{i,j: i \neq j} \{\|\widehat{\xi}_i - \widehat{\xi}_j\|_2\}}.$$

Using this normalized metric, we construct Wasserstein ambiguity sets and evaluate the sensitivity of dr-SAGHP for radii ranging from 0 to 1.

5.4 Numerical Results

5.4.1 Computational performance

We begin by assessing the computational performance of the proposed approach in Section 4.4, which integrates Kelly’s cutting plane procedure into an integer L-shaped approach. We refer to this method as K-IL. Using the empirical joint capacity distributions constructed in Section 5.2, we solve dr-SAGHP via both K-IL and by direct solution of the deterministic equivalent formulation of dr-SAGHP (problem (28)) using Gurobi. We refer to the latter method as DE. The numerical results are reported in Table 2. As shown therein, K-IL consistently requires substantially less computation time than DE, providing solution times that are 12.87 times to 102.25 times faster. Notably, once ε exceeds 0.6, the objective value plateaus, i.e., enters an ε -insensitive saturation regime. This indicates that for sufficiently large Wasserstein radii, the same worst-case distribution within the ambiguity set remains optimal, so further enlarging ε no longer affects the objective. Consequently, before saturation, K-IL is up to 25 times faster; after saturation, the relative speedup becomes even more pronounced, exceeding 100 times in our experiments. Moreover, the resulting optimality gaps remain negligible—ranging from 0 to 0.063%—indicating that the proposed integer L-shape method attains near-optimal objective values while offering a significant improvement in computational efficiency.

5.4.2 In-sample performance

Furthermore, Figure 1 reports the resulting *in-sample* performance. When evaluated under the empirical joint capacity distribution from the fitted GPR, the in-sample cost of dr-SAGHP increases monotonically with the Wasserstein radius ε , indicating that the dr-SAGHP solutions become increasingly conservative as the ambiguity set expands and the greater distributional robustness leads to

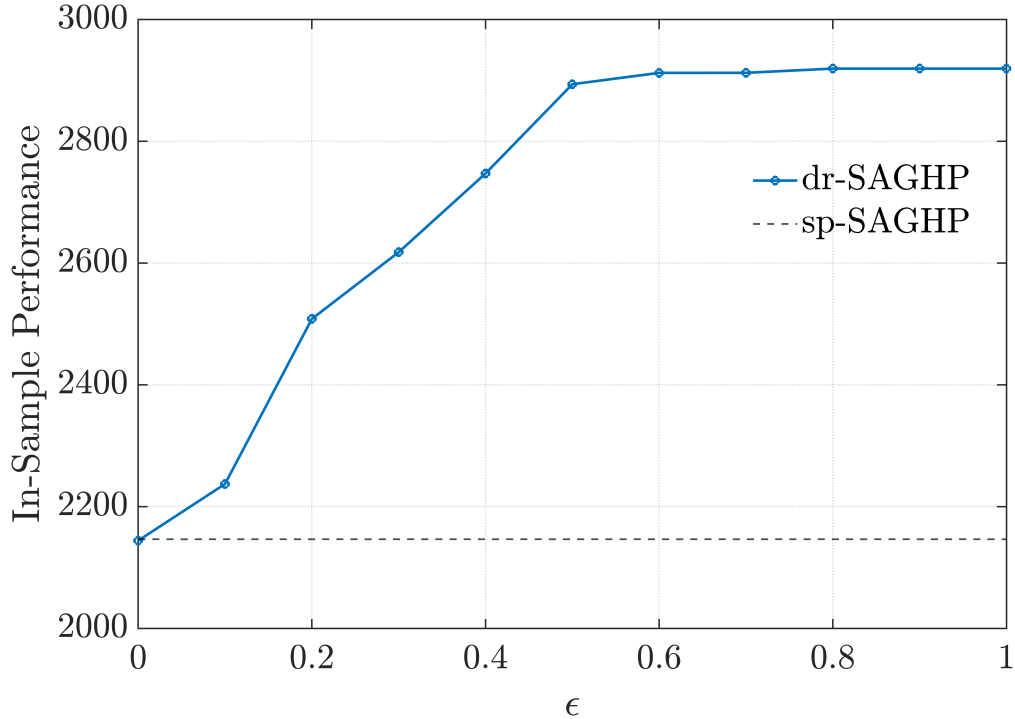


Figure 1: In-sample performance of sp-SAGHP and dr-SAGHP with various epsilons.

deteriorated in-sample performance. Note that when $\varepsilon = 0$, the Wasserstein ball collapses to a singleton containing only the empirical joint distribution. Consequently, the dr-SAGHP model coincides with the s-SAGHP model, and their in-sample costs are identical. This is expected, as the s-SAGHP minimizes the in-sample expected value, while the dr-SAGHP minimizes a different objective.

5.4.3 Out-of-Sample performance

For the out-of-sample evaluation under both mean-reduction and variance-increase stressors, we generate 1,000 perturbed capacity trajectories after altering either the mean or covariance of the GPR-implied distribution (i.e., $\tilde{\psi} \sim \mathcal{N}(\tilde{\mu}_r, \tilde{\Sigma}_\gamma)$), and we compute the corresponding realized cost $\Phi(x, \tilde{\psi})$ as well as the risk metric $\text{CVaR}_\tau(\Phi(x, \tilde{\psi}))$. We note that we use the 1,000 generated trajectories to approximate the integral in Equation (23) when evaluating CVaR.

Turning to the mean-reduction experiments (Figures 2a–3d), dr-SAGHP consistently outperforms s-SAGHP across all reduction levels on both expected costs and CVaR (the small discrepancy between s-SAGHP and dr-SAGHP at $\varepsilon = 0$ is attributable to numerical tolerances). Under a mild reduction ($r = 0.05$, Figure 2a), the out-of-sample cost initially decreases with ε and attains its minimum at $\varepsilon = 0.2$, after which performance deteriorates as ε continues to increase. As the reduction becomes more severe (Figures 2b–2d), dr-SAGHP remains uniformly superior, and the gains become more pronounced. Specifically, relative to s-SAGHP, the best-performing dr-SAGHP (at ε^*) achieves out-of-sample expected cost reductions of 11.00%, 24.77%, 27.20%, and 24.17% for $r = 0.05, 0.10, 0.15,$ and 0.20 , respectively (Table 3). As for out-of-sample CVaR, dr-SAGHP achieves consistent reductions of at least 19.08% for all mean reduction levels (Table 4).

As for the variance-increase experiments, we evaluate out-of-sample expected costs across covariance inflation levels, with the posterior covariance scaled by $(1 + \gamma)$ for $\gamma \in \{0.5, 1.0, 1.5, 2.0\}$ and CVaR_τ across tail levels $\tau \in \{0.01, 0.05, 0.1, 0.15, 0.20\}$ (Figures 4a–5d). For both s-SAGHP and dr-SAGHP, holding τ fixed, larger variance increases (larger γ) consistently lead to higher operating costs. Moreover, for a fixed γ , smaller τ yields larger CVaR_τ values than larger τ , as expected since smaller τ focuses on more extreme tail outcomes.

In terms of model comparison, dr-SAGHP consistently outperforms s-SAGHP across all (γ, τ) combinations in CVaR. As shown in Table 6, under a mild variance increase ($\gamma = 0.5$), the best-

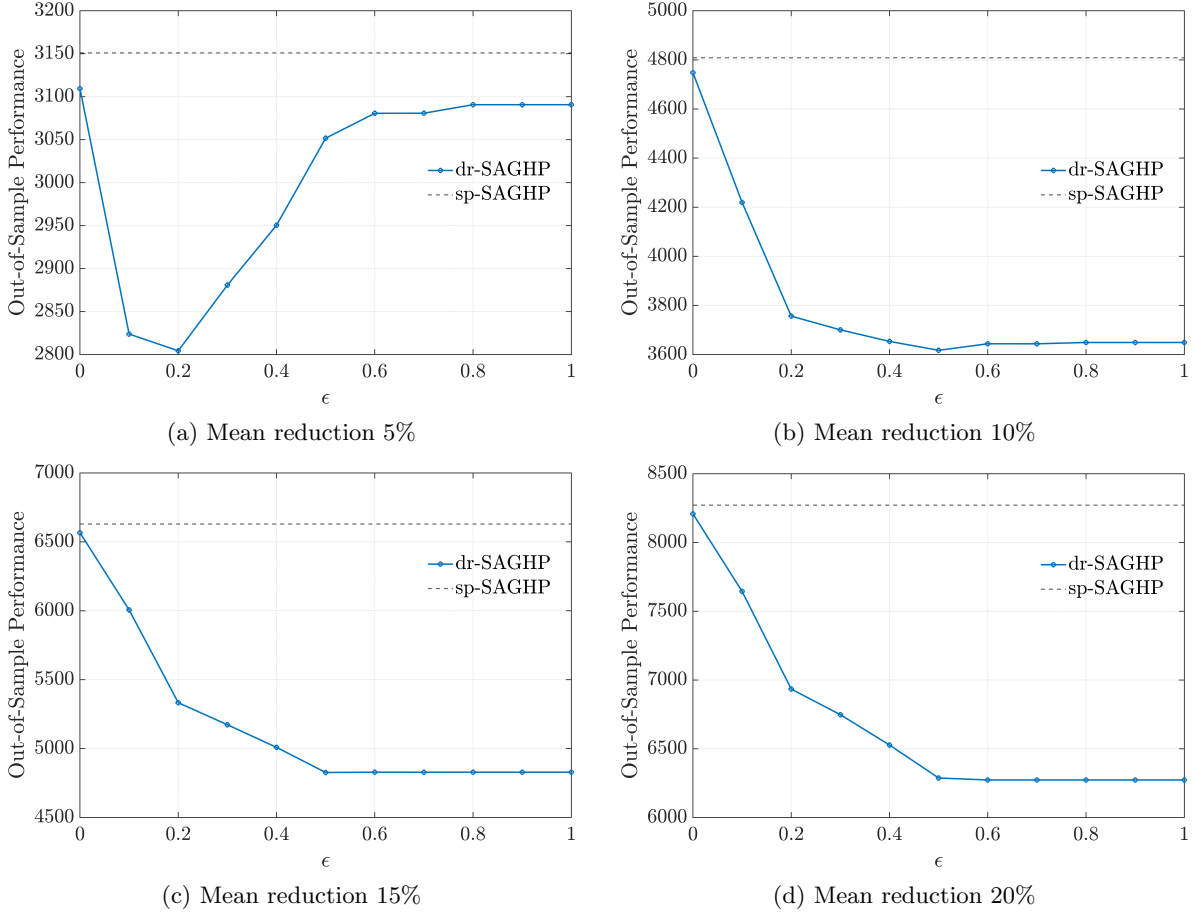


Figure 2: Out-of-sample performance comparison in expected costs between dr-SAGHP and s-SAGHP under different levels of mean reduction.

performing dr-SAGHP (at ϵ^*) reduces operating cost by approximately 11.10%–26.00% relative to s-SAGHP; under a more severe variance increase ($\gamma = 2.0$), the reduction ranges from 15.33% to 24.44%. The advantage of dr-SAGHP is most pronounced for smaller τ , and diminishes as τ increases, indicating that distributional robustness is particularly beneficial for mitigating extreme tail-risk outcomes. As γ increases, the relative gains at larger τ become more noticeable, suggesting that robustness becomes increasingly valuable as predictive uncertainty grows. Finally, we observe that larger τ generally favors smaller optimal radii ϵ^* (e.g., $\epsilon^* = 0.2$ for $\tau \geq 0.15$ across all γ), whereas smaller τ tends to select larger ϵ^* (e.g., $\epsilon^* = 0.5$ for $\tau = 0.01$), consistent with the need for larger ambiguity sets when emphasizing extreme-tail performance.

Table 5 also shows that, for mild variance inflation (e.g., $\gamma = 0.5$ and $\gamma = 1.0$), s-SAGHP attains slightly lower expected costs than dr-SAGHP. This behavior is expected because the variance-increase experiments preserve the out-of-sample mean while only amplifying dispersion. Nevertheless, dr-SAGHP remains attractive: despite at most a 1.71% increase in expected cost relative to s-SAGHP, it delivers substantial protection in the tail, reducing CVaR by up to 26% under adverse conditions.

5.5 Key Findings of Computational Experiments

In summary, the experiments yields four key insights. First, the in-sample behavior of dr-SAGHP matches the theoretical role of Wasserstein ambiguity sets: as the radius ϵ increases, the ambiguity set expands and the optimal decisions become more conservative, which leads to a monotone increase in in-sample cost. Second, under out-of-sample distribution shifts driven by mean reductions in airport capacity, dr-SAGHP consistently outperforms s-SAGHP, and the performance gains become larger as the capacity drop becomes more severe (e.g., from an 11% reduction at $r = 0.05$ to a 24.17% reduction at $r = 0.20$). Third, under variance-increase sensitivity analysis, dr-SAGHP also delivers robust tail

Reduction Level (r)	s-SAGHP	Best dr-SAGHP	Reduction (%)	ε^*
0.05	3278.6	2854.8	12.93%	0.20
0.10	4806.6	3617.2	24.75%	0.50
0.15	6507.3	4727.2	27.36%	0.50
0.20	8304.0	6298.9	24.15%	0.70

Table 3. Best out-of-sample expected-cost comparison across mean reduction levels. For each r , we report the best dr-SAGHP over ε and the corresponding ε^* .

Reduction Level (r)	τ	s-SAGHP	Best dr-SAGHP	Reduction (%)	ε^*
0.05	0.01	5899.0	4196.8	28.86%	0.50
0.05	0.05	5331.3	3803.9	28.65%	0.50
0.05	0.10	5045.1	3623.1	28.19%	0.50
0.05	0.15	4849.2	3517.0	27.47%	0.50
0.05	0.20	4691.2	3442.2	26.62%	0.50
0.10	0.01	7826.2	5808.4	25.78%	0.50
0.10	0.05	7137.8	5217.5	26.90%	0.50
0.10	0.10	6800.7	4891.2	28.08%	0.50
0.10	0.15	6583.6	4689.0	28.78%	0.50
0.10	0.20	6417.7	4528.6	29.44%	0.50
0.15	0.01	9496.5	7364.5	22.45%	0.50
0.15	0.05	8777.3	6752.0	23.07%	0.50
0.15	0.10	8420.2	6456.2	23.32%	0.50
0.15	0.15	8192.8	6267.9	23.50%	0.50
0.15	0.20	8020.7	6127.6	23.60%	0.50
0.20	0.01	11283.1	9131.4	19.08%	0.80
0.20	0.05	10687.8	8567.2	19.84%	0.80
0.20	0.10	10318.6	8191.6	20.61%	0.80
0.20	0.15	10078.6	7967.0	20.95%	0.80
0.20	0.20	9887.5	7781.3	21.30%	0.80

Table 4. Best out-of-sample CVaR comparison across mean reduction levels. For each (r, τ) , we report the best dr-SAGHP over ε and the corresponding ε^* .

Variance Increase (γ)	s-SAGHP	Best dr-SAGHP	Reduction (%)	ε^*
0.5	2302.2	2341.6	-1.71%	0.10
1.0	2457.3	2464.3	-0.29%	0.10
1.5	2560.7	2547.9	0.50%	0.10
2.0	2669.7	2648.6	0.79%	0.10

Table 5. Best out-of-sample expected-cost comparison across variance increase levels, excluding $\varepsilon = 0$. For each γ , we report the best dr-SAGHP over $\varepsilon > 0$ and the corresponding ε^* .

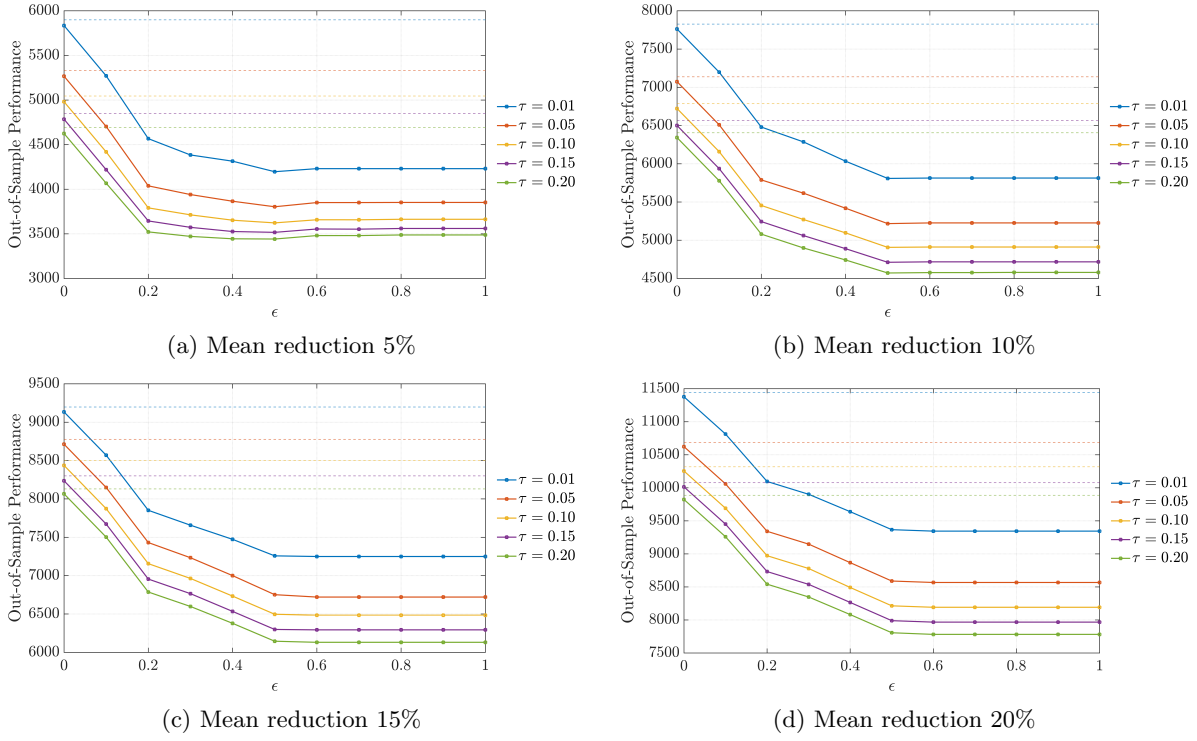


Figure 3: Out-of-sample performance comparison in CVAR between dr-SAGHP and s-SAGHP under different levels of mean reduction.

performance, reducing out-of-sample CVaR_τ by up to 26% relative to s-SAGHP; moreover, as predictive uncertainty grows, the optimal robustness level typically shifts toward larger ambiguity radii. Fourth, these results suggest a practical guideline for deployment: when deviations from historical capacity distribution are mild, s-SAGHP (or dr-SAGHP with a small ε) is often sufficient and avoids unnecessary conservatism, whereas under distributional shifts, enlarging the ambiguity set is essential for strong out-of-sample performance. Consequently, selecting ε entails a fundamental trade-off between conservativeness and robustness.

Overall, these findings indicate that dr-SAGHP adapts effectively across uncertainty regimes, imposing minimal conservatism under mild shifts while delivering substantial performance improvements under severe climate change impacted scenarios.

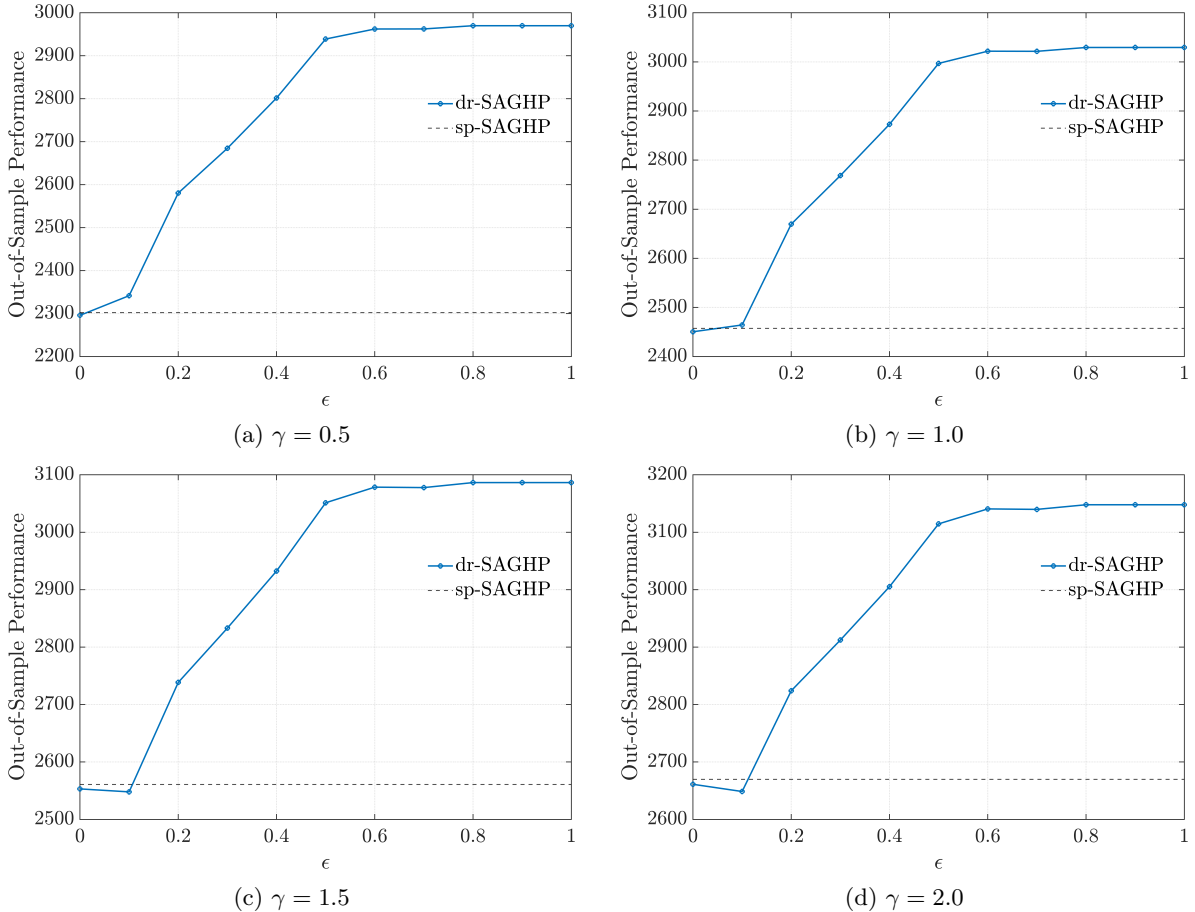


Figure 4: Out-of-sample performance comparison in expected cost between dr-SAGHP and s-SAGHP under different levels of capacity variance increase.

6 Conclusion

In this paper, we proposed a distributionally robust framework for optimizing single-airport ground holding policies (dr-SAGHP) to deal with uncertain airport capacity distributions caused by climate change. Building on classical GDP formulations and stochastic programming approaches, our work addresses a key practical limitation of stochastic programming models: their reliance on an accurately specified probability distribution of airport capacity. In operational environments where capacity distributions are highly variable, poorly estimated, or subject to abrupt structural shifts (e.g., due to severe weather), such assumptions are often unrealistic.

To overcome this challenge, we apply a Distributionally Robust Optimization framework with a discrete Wasserstein ambiguity set, and derive the Two-Stage Distributionally Robust Single Airport Ground Holding Problem and its tractable convex reformulation according to the standard procedure in [Esfahani and Peyman, 2018]. We further develop a method that applies Kelly’s cutting plane within an integer L-shaped method. Utilizing the structure of two-stage distributionally robust integer program with relatively complete recourse and continuous second-stage decision variables, we develop a fast algorithm for computing the subgradients required by Kelly’s cutting plane method. Our computational study shows that this algorithm achieves substantial speedup compared with the tractable convex reformulation: from 12.87 to 102.25 times faster while maintaining extremely small optimality gaps (between 0.000% and 0.063%). This demonstrates that the proposed algorithm is both scalable and highly accurate.

In order to evaluate the performance of dr-SAGHP under the impacts of climate change, we simulate airport capacity scenarios and then conduct sensitivity analysis on them. We apply Gaussian Process Regression to fit historical weather factors and airport capacity data at EWR from 2021 to 2022, generating airport capacity scenarios. We simulate two cases, mean reductions and variance

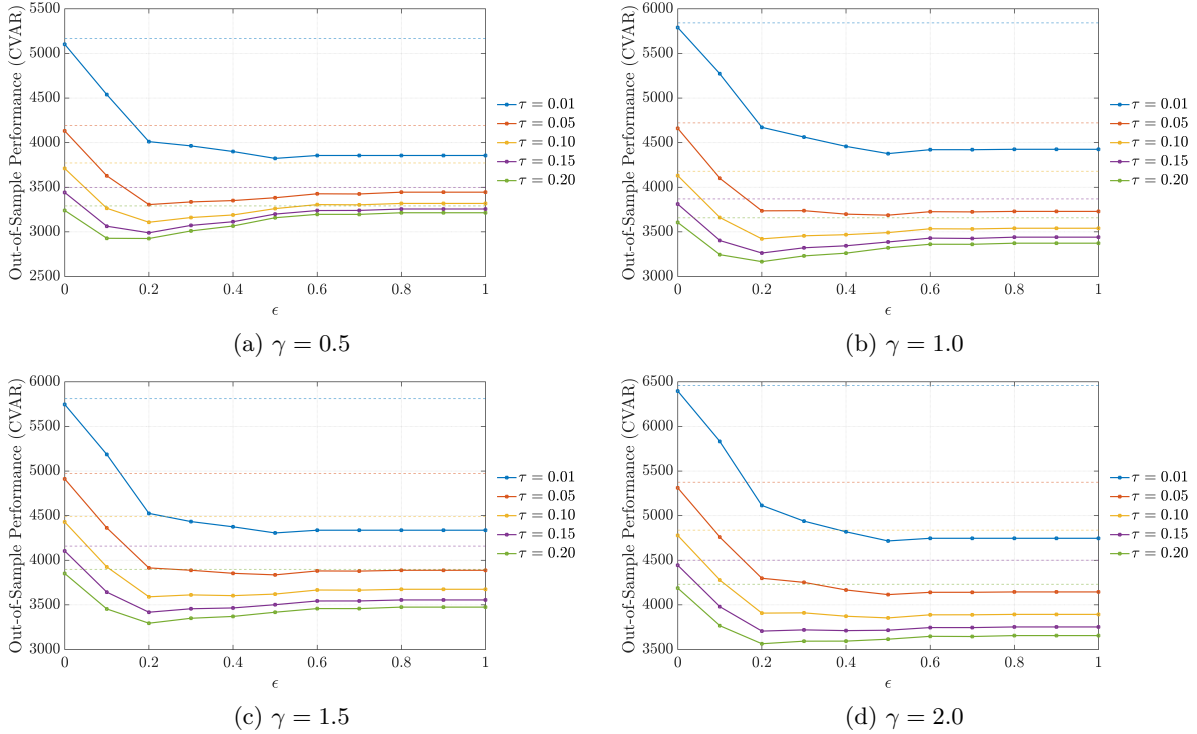


Figure 5: Out-of-sample performance comparison in CVAR between dr-SAGHP and s-SAGHP under different levels of capacity variance increase.

increase in airport capacity distributions, by perturbing mean vector and covariance matrix of the posterior distribution from the fitted GPR. The sensitivity analysis demonstrates that dr-SAGHP save more than 20% operation costs when there exists more than 10% mean reduction in airport capacity distribution caused by climate change. As for variance increase, dr-SAGHP could mitigate the risk from 11.10% to 26% when evaluated on CVaR and on various variance increase levels and confidence levels. These findings provide a clear operational guideline: when capacity conditions are stable or only mildly perturbed, the SP or low- ϵ dr-SAGHP model is adequate and avoids unnecessary conservatism; however, under moderate-to-severe distribution shifts, enlarging the ambiguity set yields substantial performance gains. This highlights the fundamental trade-off between robustness and efficiency in real-world deployment.

Overall, our results show that the proposed dr-SAGHP offers a flexible and resilient decision-making framework that remains effective even when the true airport capacity distribution is uncertain, poorly estimated, or subject to significant disruption caused by climate change. The combination of theoretical tractability, algorithmic efficiency, and strong empirical performance suggests that DRO-based ground delay program can serve as a powerful tool for enhancing the resilience of air transportation systems.

There are several natural directions in which this work can be extended. One promising avenue is to apply the proposed distributionally robust framework and integer L-shaped algorithm to the multi-airport ground holding problem, where airport operations are coupled through shared airspace, weather systems, and network-level traffic flow interactions. Incorporating joint capacity distributions across the FAA Core 30 airports—and explicitly modeling the statistical dependencies between airport capacities—would provide a more realistic representation of the National Airspace System and enable more coordinated delay management strategies.

Another important extension involves moving beyond the static ground delay formulation used in this study. In practice, airport capacity forecasts evolve over time as weather conditions, demand patterns, and upstream congestion unfold. A multi-stage distributionally robust ground delay model would allow ground delay decisions to be updated dynamically as new information becomes available. Developing such a framework requires integrating multi-stage DRO with tractable decomposition or approximation techniques, with the goal of enabling real-time or near-real-time decision support in operational settings.

Variance Increase (γ)	τ	s-SAGHP	Best dr-SAGHP	Reduction (%)	ε^*
0.5	0.01	5166.7	3823.6	26.00%	0.50
0.5	0.05	4193.0	3305.9	21.16%	0.20
0.5	0.10	3771.9	3107.9	17.61%	0.20
0.5	0.15	3497.9	2989.7	14.53%	0.20
0.5	0.20	3290.9	2925.7	11.10%	0.20
1.0	0.01	5842.6	4377.4	25.08%	0.50
1.0	0.05	4721.9	3687.3	21.91%	0.50
1.0	0.10	4179.6	3421.7	18.13%	0.20
1.0	0.15	3869.0	3262.9	15.67%	0.20
1.0	0.20	3657.0	3166.3	13.42%	0.20
1.5	0.01	6503.2	4895.1	24.73%	0.50
1.5	0.05	5268.4	4112.3	21.94%	0.50
1.5	0.10	4666.1	3790.3	18.77%	0.50
1.5	0.15	4318.6	3590.5	16.86%	0.20
1.5	0.20	4079.3	3464.7	15.07%	0.20
2.0	0.01	7146.7	5399.9	24.44%	0.50
2.0	0.05	5797.1	4532.2	21.82%	0.50
2.0	0.10	5119.5	4162.8	18.69%	0.50
2.0	0.15	4727.4	3925.3	16.97%	0.20
2.0	0.20	4454.7	3771.7	15.33%	0.20

Table 6. Best out-of-sample CVaR performance comparison across variance increase levels. For each (γ, τ) , we report the best dr-SAGHP over ε and the corresponding ε^* .

Advancing the model along these directions would significantly enhance its practical applicability, bringing distributionally robust ground delay optimization closer to deployment in real-world air transportation systems.

References

- A. Agustí, Antonio Alonso-Ayuso, Laureano F. Escudero, and Celeste Pizarro. On air traffic flow management with rerouting. part ii: Stochastic case. *European Journal of Operational Research*, (1), 2012.
- G. Andreatta and L. Brunetta. Multi-airport ground holding problem: A computational evaluation of exact algorithms. *Operations Research*, 46(1):57–64, 1998.
- G. Andreatta and G. Tidona. A new formulation for the multi-airport ground holding problem. *University of Padova, Tech. Rep.*, 1994.
- Michael O. Ball, Robert Hoffman, Amedeo R. Odoni, and Ryan Rifkin. A stochastic integer program with dual network structure and its application to the ground-holding problem. *Operations research*, 51(1):167–171, 2003.
- Dimitri P Bertsekas. *Control of uncertain systems with a set-membership description of the uncertainty*. PhD thesis, Massachusetts Institute of Technology, 1971.
- Dimitris Bertsimas and John N Tsitsiklis. *Introduction to linear optimization*, volume 6. Athena scientific Belmont, MA, 1997.
- Kieran Bhatia, Alexander Baker, Wenchang Yang, Gabriel Vecchi, Thomas Knutson, Hiroyuki Murakami, James Kossin, Kevin Hodges, Keith Dixon, Benjamin Bronselaer, and Carolyn Whitlock. A potential explanation for the global increase in tropical cyclone rapid intensification. *Nature communications*, 13(1):6626, 2022.

- John R Birge and Francois Louveaux. *Introduction to stochastic programming*. Springer, 1997.
- Bureau of Transportation Statistics. Airline on-time performance data, 2026.
- J. Chen, Chen L., and D. Sun. Air traffic flow management under uncertainty using chance-constrained optimization. *Transportation Research Part B: Methodological*, 102:124–141, 2017.
- Jun Chen and Dengfeng Sun. Stochastic ground-delay-program planning in a metroplex. *Journal of Guidance, Control, and Dynamics*, 41(1):231–239, 2018.
- Sun Choi and Young Jin Kim. Artificial neural network models for airport capacity prediction. *Journal of Air Transport Management*, 2021.
- Ben Clarke, Friederike Otto, Rupert Stuart-Smith, and Luke Harrington. Extreme weather impacts of climate change: an attribution perspective. *Environmental Research: Climate*, 1(1):012001, 2022.
- Luca Corolli, Guglielmo Lulli, Lewis Ntaimo, and Saravanan Venkatachalam. A two-stage stochastic integer programming model for air traffic flow management. *IMA Journal of Management Mathematics*, 28(1):19–40, 2017.
- Victor Hugo Souza de Abreu, Andrea Souza Santos, and Thaís Guedes Máximo Monteiro. Climate change impacts on the road transport infrastructure: A systematic review on adaptation measures. *Sustainability*, 14(14):8864, 2022.
- Erick Delage and Yinyu Ye. Distributionally robust optimization under moment uncertainty with application to data-driven problems. *Operations research*, 58(3):595–612, 2010.
- Shahab Doulabian, Erfan Ghasemi Tousi, Amirhossein Shadmehri Toosi, and Sina Alaghmand. Non-stationary precipitation frequency estimates for resilient infrastructure design in a changing climate: A case study in sydney. *Hydrology*, 10(6):117, 2023.
- Mohajerin Esfahani and Daniel Kuhn Peyman. Data-driven distributionally robust optimization using the wasserstein metric: Performance guarantees and tractable reformulations. *Mathematical Programming*, 171(1-2):115–166, 2018.
- Alexander S. Estes and Michael O. Ball. Equity and strength in stochastic integer programming models for the dynamic single airport ground-holding problem. *Transportation Science*, 54(4):944–955, 2020.
- FAA. Traffic flow management in the national airspace system. 2009.
- Davide Faranda, Stella Bourdin, Mireia Ginesta, Meriem Krouma, Gabriele Messori, Robin Noyelle, Flavio Pons, and Pascal Yiou. A climate-change attribution retrospective of some impactful weather extremes of 2021. *Weather and Climate Dynamics Discussions*, 2022:1–37, 2022.
- Federal Aviation Administration. Airport capacity profiles. Web page, 2026a. URL https://www.faa.gov/airports/planning_capacity/profiles. Accessed: 2026-01-29.
- Federal Aviation Administration. Aspm weather factors: Details report. ASPMHelp (web documentation), 2026b. URL https://www.aspm.faa.gov/aspmhelp/index/ASPM_Weather_Factors_Details_Report.html. Accessed: 2026-01-29.
- Charles N. Glover and Michael O. Ball. Stochastic optimization models for ground delay program planning with equity–efficiency tradeoffs. *Transportation Research Part C: Emerging Technologies*, pages 196–202, 2013.
- Shubham Gupta and Dimitris J. Bertsimas. Multistage air traffic flow management under capacity uncertainty: a robust and adaptive optimization approach. *European Journal of Operational Research*, 2011.
- David Jaroszweski, Elizabeth Hooper, and Lee Chapman. The impact of climate change on urban transport resilience in a changing world. *Progress in Physical Geography*, 38(4):448–463, 2014.

- J. E. Kelley, Jr. The cutting-plane method for solving convex programs. *Journal of the Society for Industrial and Applied Mathematics*, 8(4):703–712, 1960. doi: 10.1137/0108053. URL <https://doi.org/10.1137/0108053>.
- Rafal Kicinger, Jit-Tat Chen, Matthias Steiner, and James Pinto. Airport capacity prediction with explicit consideration of weather forecast uncertainty. *Journal of Air Transportation*, 24(1):18–28, 2016.
- Gilbert Laporte and François V. Louveaux. The integer l-shaped method for stochastic integer programs with complete recourse. *Operations Research Letters*, 13(3):133–142, 1993. ISSN 0167-6377. doi: [https://doi.org/10.1016/0167-6377\(93\)90002-X](https://doi.org/10.1016/0167-6377(93)90002-X). URL <https://www.sciencedirect.com/science/article/pii/016763779390002X>.
- Subhra Sekhar Maity and Rajib Maity. Changing pattern of intensity–duration–frequency relationship of precipitation due to climate change. *Water Resources Management*, 36(14):5371–5399, 2022.
- Samuel A Markolf, Christopher Hoehne, Andrew Fraser, Mikhail V Chester, and B Shane Underwood. Transportation resilience to climate change and extreme weather events–beyond risk and robustness. *Transport policy*, 74:174–186, 2019.
- Arpita Mondal and PP Mujumdar. Hydrologic extremes under climate change: non-stationarity and uncertainty. In *Sustainable water resources planning and management under climate change*, pages 39–60. Springer, 2016.
- Laura Moretti and Giuseppe Loprencipe. Climate change and transport infrastructures: State of the art. *Sustainability*, 10(11):4098, 2018.
- Avijit Mukherjee and Mark Hansen. Dynamic stochastic optimization model for air traffic flow management with en route and airport capacity constraints. *Proc. 6th USA/Eur. Air Traffic Manage. R&D Seminar.*, 2005.
- Avijit Mukherjee and Mark Hansen. A dynamic stochastic model for the single airport ground holding problem. *Transportation Science*, 41(4):444–456, 2007.
- Mayara Condé Rocha Murça and R John Hansman. Predicting and planning airport acceptance rates in metroplex systems for improved traffic flow management decision support. *Transportation Research Part C: Emerging Technologies*, 97:301–323, 2018.
- Masahiko Nagai and Arnob Bormudoi. A spatiotemporal analysis of heterogeneity and non-stationarity of extreme precipitation in the ayeyarwady river basin, myanmar, and their linkages to global climate variability. *Water*, 18(2):227, 2026.
- Richard de Neufville, Amedeo R. Odoni, Peter P. Belobaba, and Tom G.s Reynolds. Airport systems: Planning, design, and management. 2013.
- Octavio Richetta and Amedeo R. Odoni. Solving optimally the static ground-holding policy problem in air traffic control. *Transportation Science*, 27(3):228–238, 1993.
- R Tyrrell Rockafellar and Stanislav Uryasev. Optimization of conditional value-at-risk. *Journal of risk*, 2:21–42, 2000.
- CJiang Ruiwei, Minseok Ryu, and Guanglin Xu. Data-driven distributionally robust appointment scheduling over wasserstein ball. *arXiv preprint*, 2019.
- Tim Ryley, Stefan Baumeister, and Liese Coulter. Climate change influences on aviation: A literature review. *Transport Policy*, 92:55–64, 2020.
- Alexander Shapiro, Darinka Dentcheva, and Andrzej Ruszczyński. *Lectures on stochastic programming: modeling and theory*. SIAM, 2021.
- Ottar Tamm, Egle Saaremäe, Kristiina Rahkema, Jaak Jaagus, and Toomas Tamm. The intensification of short-duration rainfall extremes due to climate change–need for a frequent update of intensity–duration–frequency curves. *Climate services*, 30:100349, 2023.

P.B Vranas, D.J. Bertimas, and A.R. Odoni. The multi-airport ground-holding problem in air traffic control. *Operations Research*, 42(2):249–261, 1994.

Christopher Williams and Carl Rasmussen. Gaussian processes for regression. *Advances in neural information processing systems*, 8, 1995.

Jianzhe Zhen, Daniel Kuhn, and Wolfram Wiesemann. Mathematical foundations of robust and distributionally robust optimization. *arXiv preprint arXiv:2105.00760*, 2021.

Yaoming Zhou, Junwei Wang, and Hai Yang. Resilience of transportation systems: concepts and comprehensive review. *IEEE Transactions on Intelligent Transportation Systems*, 20(12):4262–4276, 2019.

Wang Ziming, Chaohao Liao, Xu Hang, Lishuai Li, Daniel Delahaye, and Mark Hansen. Distribution prediction of strategic flight delays via machine learning methods. *Sustainability* 14, 14(22):15186, 2022.

A Derivation of deterministic formulation of dr-SAGHP

The steps are shown as follow:

Step 1: Substitute the discrete Wasserstein ambiguity set. We begin by substituting the discrete Wasserstein ambiguity set into the inner maximization problem in (6). The ambiguity set can be written as

$$\mathcal{P}_\varepsilon(\hat{p}) := \left\{ p \in \mathbb{R}^{|\Xi|} : W(\hat{p}, p) \leq \varepsilon \right\} \\ = \left\{ p \in \mathbb{R}^{|\Xi|} : \exists \pi \in \mathbb{R}^{|\Xi| \times |\Xi|} \text{ s.t. } \begin{cases} \sum_{i=1}^{|\Xi|} \sum_{j=1}^n \pi_{i,j} d_{i,j} \leq \varepsilon, \\ \sum_{j=1}^{|\Xi|} \pi_{i,j} = \hat{p}_i, \quad \forall i, \\ \sum_{i=1}^{|\Xi|} \pi_{i,j} = p_j, \quad \forall j, \\ \pi_{i,j} \geq 0, \quad \forall i, j, \end{cases} \right\}. \quad (24)$$

The variable $\pi_{i,j}$ is a nonnegative transportation plan indicating the amount of probability mass moved from support point i of \hat{P} to support point j of P .

Step 2: Rewrite the worst-case expectation as a dual linear program in Π . By integrating (24) into the inner maximization problem of (3.2), we obtain

$$\max_{p \in \mathcal{P}_\varepsilon(\hat{p})} \mathbb{E}_p[Q(x, \xi)] = \max_{\pi \in [0,1]^{|\Xi| \times |\Xi|}} \sum_{i=1}^{|\Xi|} \sum_{j=1}^{|\Xi|} \pi_{i,j} Q(x, \xi_j) \quad (25a)$$

$$\text{s.t. } \sum_{i=1}^{|\Xi|} \sum_{j=1}^{|\Xi|} \pi_{i,j} d_{i,j} \leq \varepsilon, \quad (25b)$$

$$\sum_{j=1}^{|\Xi|} \pi_{i,j} = \hat{p}_i, \quad \forall i \in \{1, \dots, |\Xi|\} \quad (25c)$$

$$\sum_{i=1}^{|\Xi|} \pi_{i,j} = p_j, \quad \forall j \in \{1, \dots, |\Xi|\} \quad (25d)$$

$$\pi_{i,j} \geq 0, \quad \forall i, j \in \{1, \dots, |\Xi|\} \quad (25e)$$

For notational convenience, we substitute $p_j = \sum_{i=1}^n \pi_{i,j}$ to eliminate p . We then take the standard dual form of this linear program and have

$$\min_{\lambda \in \mathbb{R}^{|\Xi|}, \alpha \in \mathbb{R}^{|\Xi| \times |\Xi|}} \lambda \varepsilon + \sum_{i=1}^n \alpha_i \widehat{p}_i \quad (26a)$$

$$\text{s.t. } \alpha_i + \lambda d_{i,j} \geq Q(x, \xi_j), \quad \forall i, j, \quad (26b)$$

$$\lambda \geq 0. \quad (26c)$$

Step 3: Substitute the dual into the first-stage problem. By strong duality of linear programming, (??) is equivalent to the primal inner maximization (25). Substituting (??) into (6), dr-SAGHP can be equivalently rewritten as

$$\min_x \left\{ \sum_{f \in F} C_f \left(\sum_{t \in T_f} t x_{f,t} - r_f \right) + \min_{\lambda \geq 0, \alpha} \lambda \varepsilon + \sum_{i=1}^n \alpha_i \widehat{p}_i \right\} \quad (27a)$$

$$\text{s.t. } (1c), (1d), (1e), (??) \quad (27b)$$

Since the first-stage objective is independent of (λ, α) , the objective can be written equivalently as

$$\min_{x, \lambda \geq 0, \alpha} \sum_{f \in F} C_f \left(\sum_{t \in T_f} t x_{f,t} - r_f \right) + \lambda \varepsilon + \sum_{i=1}^n \widehat{p}_i \alpha_i.$$

Step 4: Deterministic equivalent formulation. Combining the above and collecting decision variables, as well as substituting the explicit definition of the second-stage value function $Q(x, \widehat{\xi}_j)$ from (3) yields the deterministic equivalent formulation:

$$\min_{x, \lambda, \alpha} \left\{ \sum_{f \in F} C_f \left(\sum_{t \in T_f} t x_{f,t} - r_f \right) + \lambda \varepsilon + \sum_{i=1}^n \alpha_i \widehat{p}_i \right\} \quad (28a)$$

$$\text{s.t. } \alpha_i + \lambda d_{i,j} \geq \sum_{t \in T} C_h y_t(\xi_j), \quad \forall i, j \in \{1, \dots, |\Xi|\} \quad (28b)$$

$$y_t(\xi) - y_{t-1}(\xi) \geq \sum_{f \in F} x_{f,t} - K_t(\xi), \quad \forall t \in T, \xi \in \Xi, \quad (28c)$$

$$y_0(\xi) \geq \sum_{f \in F} x_{f,0} - K_0(\xi), \quad \forall \xi \in \Xi, \quad (28d)$$

$$\sum_{t \in T_f} x_{f,t} = 1, \quad \forall f \in F, \quad (28e)$$

$$\begin{aligned} & \sum_{t \in T_{f_2}} t x_{f_2,t} - r_{f_2} \\ & \geq \sum_{t \in T_{f_1}} t x_{f_1,t} - r_{f_1} - S_{f_1, f_2}, \quad f_1, f_2 \in \mathcal{C}, \end{aligned} \quad (28f)$$

$$y_t(\xi) \geq 0, \quad \forall f \in F, t \in T, \xi \in \Xi, \quad (28g)$$

$$x_{f,t} \in \{0, 1\}, \forall f \in F, t \in T \quad (28h)$$

$$\lambda \geq 0 \quad (28i)$$

B Proof of Proposition 4.1

Proposition 4.1 follows from an application of Danskin's Theorem. We use a variant from Bertsekas [1971]:

Theorem B.1 (Danskin's Theorem Bertsekas [1971]). *Let $\mathbf{g} : \mathbb{R}^n \times \mathbb{R}^m \rightarrow (-\infty, \infty)$ be a function and let \mathbf{Y} be a compact subset of \mathbb{R}^m . Assume further that for every vector $\mathbf{y} \in \mathbf{Y}$ the function $\mathbf{g}(\cdot, \mathbf{y}) : \mathbb{R}^n \rightarrow (-\infty, \infty)$ is a closed proper convex function. Consider the function \mathbf{f} defined as $\mathbf{f}(\mathbf{x}) = \sup_{\mathbf{y} \in \mathbf{Y}} \mathbf{g}(\mathbf{x}, \mathbf{y})$, if $\text{int}(\text{dom } \mathbf{f}) \neq \emptyset$ and \mathbf{g} is continuous on the set $\text{int}(\text{dom } \mathbf{f}) \times \mathbf{Y}$ for every $\mathbf{x} \in \text{int}(\text{dom } \mathbf{f})$ we have*

$$\partial \mathbf{f}(\mathbf{x}) = \text{conv}\{\partial \mathbf{g}(\mathbf{x}, \mathbf{y}^*) | \mathbf{y}^* \in \mathbf{Y}^*(\mathbf{x})\},$$

where

$$\mathbf{Y}^*(\mathbf{x}) = \{\mathbf{y}^* \in \mathbf{Y} | \mathbf{g}(\mathbf{x}, \mathbf{y}^*) = \max_{\mathbf{y} \in \mathbf{Y}} \mathbf{g}(\mathbf{x}, \mathbf{y})\}.$$

In order to verify that the conditions of the theorem are satisfied, we must verify the following:

- The set \mathcal{P}_ε is compact. This is true, as this set is a bounded polytope.
- For each probability distribution p , the function $\mathbf{x} \mapsto \sum_{i=1}^{|\Xi|} p_i h(\mathbf{x}, \xi_i)$ is a closed proper convex function, letting this function take the value ∞ when $\mathbf{x} \notin [0, 1]^{\mathbf{N}}$. This function is closed, as it is infinite outside the unit cube $[0, 1]^{\mathbf{N}}$. The fact that it is proper and convex follows from the assumption that $h(\cdot, \xi_i)$ is convex and the assumption that $\sum_{i=1}^{|\Xi|} p_i h(\mathbf{x}, \xi_i)$ is finite for all \mathbf{x} and $p \in \mathcal{P}_\varepsilon$.
- The interior of the domain of f is non-empty. This is true as the domain of f is $[0, 1]^{\mathbf{N}}$.
- The function $(\mathbf{x}, p) \mapsto \sum_{i=1}^{|\Xi|} p_i h(\mathbf{x}, \xi_i)$ is continuous on $(0, 1)^{\mathbf{N}} \times \mathcal{P}_\varepsilon$. This can be shown to be true. Fix any i . The i th coordinate projection $p \mapsto p_i$ is linear and therefore continuous. Moreover, each recourse function $h(\cdot, \xi_i)$ is assumed to be convex, and therefore continuous on the interior of its domain. Since $h(\mathbf{x}, \xi_i)$ does not depend on p , it follows that $(\mathbf{x}, p) \mapsto h(\mathbf{x}, \xi_i)$ is continuous in (\mathbf{x}, p) on $\text{int}(\text{dom } \mathbf{f}) \times \mathcal{P}_\varepsilon$. Because the product of continuous functions is continuous, $(x, p) \mapsto p_i h(\mathbf{x}, \xi_i)$ is continuous in (x, p) on $\text{int}(\text{dom } \mathbf{f}) \times \mathcal{P}_\varepsilon$ for each i . Finally, \mathbf{g} is a finite sum of continuous functions, and is therefore continuous on $\text{int}(\text{dom } \mathbf{f}) \times \mathcal{P}_\varepsilon$.

Then, Proposition 4.1 follows immediately.

C Proof of Proposition 4.2

Let (λ, α) be a feasible solution to problem (17), and let λ^* be an optimal solution to the problem (18). Then, since (λ, α) is feasible, we have that

$$\alpha_i \geq h(\mathbf{x}, \xi_j) - \lambda d_{i,j}$$

for each $i \in \{1, \dots, |\Xi|\}$ and $j \in \{1, \dots, |\Xi|\}$. This further implies that

$$\alpha_i \geq \max_{j \in \{1, \dots, |\Xi|\}} (h(\mathbf{x}, \xi_j) - \lambda d_{i,j})$$

for each $i \in \{1, \dots, |\Xi|\}$. Then,

$$\begin{aligned} \varepsilon \lambda + \sum_{i=1}^{|\Xi|} p_i \alpha_i &\geq \varepsilon \lambda + \sum_{i=1}^{|\Xi|} p_i \max_{j \in \{1, \dots, |\Xi|\}} (h(\mathbf{x}, \xi_j) - \lambda d_{i,j}) \\ &= \phi(\lambda) \\ &\geq \phi(\lambda^*) \\ &= \varepsilon \lambda + \sum_{i=1}^{|\Xi|} p_i \alpha_i^*(\lambda^*) \end{aligned}$$

In addition, the solution $(\lambda^*, \alpha^*(\lambda^*))$ is feasible, as it follows immediately from the definition that

$$\alpha_i^*(\lambda^*) \geq h(\mathbf{x}, \xi_j) - \lambda^* d_{i,j}$$

for each $i \in \{1, \dots, |\Xi|\}$ and $j \in \{1, \dots, |\Xi|\}$. Thus, $(\lambda^*, \alpha^*(\lambda^*))$ is optimal. \square

D Proof of Proposition 4.3

Let $\lambda_{\text{hi}}^{(i)}$ and $\lambda_{\text{lo}}^{(i)}$ denote the values taken by these variables in iteration i , with $\lambda_{\text{hi}}^{(0)}$ and $\lambda_{\text{lo}}^{(0)}$ denoting the initial values. We note that $\lambda_{\text{hi}}^{(i+1)} - \lambda_{\text{lo}}^{(i+1)} = (\lambda_{\text{hi}}^{(i)} - \lambda_{\text{lo}}^{(i)})/2$. It follows by a routine induction argument that $\lambda_{\text{hi}}^{(i)} - \lambda_{\text{lo}}^{(i)} = (\lambda_{\text{hi}}^{(0)} - \lambda_{\text{lo}}^{(0)})/2^i$. Thus, if $i \geq \lceil \log_2((\lambda_{\text{hi}}^{(0)} - \lambda_{\text{lo}}^{(0)})/\delta) \rceil$, then we have that

$$\lambda_{\text{hi}}^{(i)} - \lambda_{\text{lo}}^{(i)} \leq \frac{\lambda_{\text{hi}}^{(0)} - \lambda_{\text{lo}}^{(0)}}{(\lambda_{\text{hi}}^{(0)} - \lambda_{\text{lo}}^{(0)})/\delta} = \delta < 2\delta$$

Thus, the algorithm stops in at most $\lceil \log_2((\lambda_{\text{hi}}^{(0)} - \lambda_{\text{lo}}^{(0)})/\delta) \rceil$ iterations.

Let $\lambda^{(i)} = (\lambda_{\text{lo}}^{(i-1)} + \lambda_{\text{hi}}^{(i-1)})/2$ and let $s^{(i)} = \varepsilon - \sum_{i=1}^{|\Xi|} p_i d_{ij^*(i, \lambda^{(i)})}$. In any iteration i , if $s^{(i)} = 0$, then $\lambda^{(i)} \in \arg \min_{\lambda \geq 0} \phi(\lambda)$.

If no such iteration exists, then it suffices to prove that $[\lambda_{\text{lo}}^{(i)}, \lambda_{\text{hi}}^{(i)}] \cap \arg \min_{\lambda \geq 0} \phi(\lambda)$ is non-empty for each i . This is true for $i = 0$ by definition. Assume by induction it holds for some $i \geq 0$, and consider the iteration $i + 1$. Let $\lambda^{(i+1)} = (\lambda_{\text{lo}}^{(i)} + \lambda_{\text{hi}}^{(i)})/2$. Consider the case where $s^{(i)} > 0$; we must show that there exists some $\lambda^* \in [\lambda_{\text{lo}}^{(i)}, \lambda_{\text{hi}}^{(i)}] \cap \arg \min_{\lambda \geq 0} \phi(\lambda)$. By the induction assumption, there exists some $\lambda^* \in [\lambda_{\text{lo}}^{(i)}, \lambda_{\text{hi}}^{(i)}] \cap \arg \min_{\lambda \geq 0} \phi(\lambda)$. If $\lambda^* \in [\lambda_{\text{lo}}^{(i)}, \lambda_{\text{hi}}^{(i)}]$ then we are done, so we may focus on the case that $\lambda^* > \lambda_{\text{hi}}^{(i)}$. Furthermore, since $s^{(i)}$ is a subgradient for ϕ , we have that:

$$\phi(\lambda^*) \geq \phi(\lambda_{\text{hi}}^{(i)}) + (s^{(i)})^\top (\lambda^* - \lambda_{\text{hi}}^{(i)})$$

Then, since $s^{(i)} > 0$ and $\lambda^* > \lambda_{\text{hi}}^{(i)}$, we have that

$$\phi(\lambda^*) \geq \phi(\lambda_{\text{hi}}^{(i)})$$

which would imply that $\lambda_{\text{hi}}^{(i)} \in \arg \min_{\lambda \geq 0} \phi(\lambda)$. The case where $s^{(i)} < 0$ is similar.

E Proof of Proposition 4.4

Proof. Proof Let:

$$A_i(\lambda) := \arg \max_{j \in \{1, \dots, |\Xi|\}} \{Q(\mathbf{x}, \xi_j) - \lambda d_{i,j}\} \quad (29)$$

When the maximizer is not unique, $A_i(\lambda)$ represents the set of all indices that attain the maximum value. Given that $\phi(\lambda)$ is a point-wise maximum of affine functions, we can derive its sub-differential as follows:

$$\partial\phi(\lambda) = \left\{ \varepsilon - \sum_{i=1}^{|\Xi|} \hat{p}_i \sum_{j \in A_i(\lambda)} \eta_{ij} d_{i,j} \mid \mu_{i,j} \geq 0, \sum_{j \in A_i(\lambda)} \mu_{i,j} = 1 \right\}.$$

Define $\bar{\lambda} = \max_{i \in \{1, \dots, |\Xi|\}, j \in \{1, \dots, |\Xi|\}} \{(Q(\mathbf{x}, \xi_j) - Q(\mathbf{x}, \xi_i))/d_{i,j} : d_{i,j} > 0\}$. Fix some $i \in \{1, \dots, |\Xi|\}$; then, for each $j \in \{1, \dots, |\Xi|\}$, we have that:

Case 1: if $d_{i,j} = 0$ then $\xi_i = \xi_j$ and

$$Q(\mathbf{x}, \xi_j) - \lambda d_{i,j} = Q(\mathbf{x}, \xi_i) - \lambda d_{i,i}$$

Case 2: If $d_{i,j} > 0$ and $Q(\mathbf{x}, \xi_j) \leq Q(\mathbf{x}, \xi_i)$, then

$$\begin{aligned} & Q(\mathbf{x}, \xi_j) - \bar{\lambda} d_{i,j} \\ &= Q(\mathbf{x}, \xi_j) - \frac{Q(\mathbf{x}, \xi_i) - Q(\mathbf{x}, \xi_j)}{d_{i,j}} d_{i,j} \\ &= 2Q(\mathbf{x}, \xi_j) - Q(\mathbf{x}, \xi_i) \\ &\leq Q(\mathbf{x}, \xi_j) \leq Q(\mathbf{x}, \xi_i) = Q(\mathbf{x}, \xi_i) - \lambda d_{i,i}. \end{aligned}$$

Case 3: If $d_{i,j} > 0$ and $Q(\mathbf{x}, \xi_j) \geq Q(\mathbf{x}, \xi_i)$, then

$$\begin{aligned} & Q(\mathbf{x}, \xi_j) - \bar{\lambda}d_{i,j} \\ & \leq Q(\mathbf{x}, \xi_j) - \frac{Q(\mathbf{x}, \xi_j) - Q(\mathbf{x}, \xi_i)}{d_{i,j}}d_{i,j} \\ & = Q(\mathbf{x}, \xi_i) = Q(\mathbf{x}, \xi_i) - \lambda d_{i,i}. \end{aligned}$$

In all cases, the active set $A_i(\bar{\lambda})$ contains i . Consequently, the sub-differential of $\phi(\bar{\lambda})$ includes the subgradient $\varepsilon - \sum_{i=1}^n \hat{p}_i d_{i,i} = \varepsilon$. Then, for any $\lambda > \bar{\lambda}$, we have that

$$\phi(\lambda) \geq \phi(\bar{\lambda}) + \varepsilon(\lambda - \bar{\lambda})$$

Then, since $\varepsilon > 0$, we have that $\phi(\lambda) > \phi(\bar{\lambda})$ for all $\lambda > \bar{\lambda}$. To further simplify the upper bound, note that for any $i \neq j$, $\frac{Q(\mathbf{x}, \xi_j) - Q(\mathbf{x}, \xi_i)}{d_{i,j}} \leq \frac{\max_j Q(\mathbf{x}, \xi_j) - \min_i Q(\mathbf{x}, \xi_i)}{\min_{i,j: d_{i,j} \neq 0} d_{i,j}}$. Therefore, for all $\lambda \geq \frac{\max_j Q(\mathbf{x}, \xi_j) - \min_i Q(\mathbf{x}, \xi_i)}{\min_{i,j: d_{i,j} \neq 0} d_{i,j}}$, we have that $\phi(\lambda) > \phi(\bar{\lambda})$. Thus, we complete the proof. \square \square

F Proof of Theorem (4.1)

Proof. Proof We relate primal and dual optimal solutions via complementary slackness. In the dual problem (??), the variables π_{ij} correspond to the primal transportation variables in (25). A primal-dual pair consisting of feasible solution π to problem (16) and a feasible solution (λ, α) to problem (17) is said to satisfy complementary slackness for linear programs if

$$\lambda \left(\sum_{i=1}^{|\Xi|} \sum_{j=1}^{|\Xi|} \pi_{ij} d_{ij} - \varepsilon \right) = 0, \quad (31)$$

and

$$\pi_{ij} (\alpha_i + \lambda d_{ij} - h(\mathbf{x}, \xi_j)) = 0 \quad \forall i, j \in \{1, \dots, |\Xi|\} \quad (32)$$

and it is known that the primal-dual pair π and (λ, α) are optimal if and only if complementary slackness is satisfied e.g. [Bertsimas and Tsitsiklis, 1997]. Fix an optimal solution λ^* to problem (18). We show that the plan $\hat{\pi}$ constructed by Algorithm 3 is (i) primal feasible and (ii) satisfies complementary slackness with $(\lambda^*, \alpha^*(\lambda^*))$. It then follows from Proposition 4.2 that $\hat{\pi}$ is primal optimal for problem (16).

We now verify feasibility and complementary slackness for $\hat{\pi}$, distinguishing two cases.

Case 1: $\lambda^* > 0$. Let π^* be an optimal solution to problem (25). By the complementary slackness condition (31), the primal optimum π^* satisfies:

$$\sum_{i=1}^{|\Xi|} \sum_{j=1}^{|\Xi|} \pi_{ij}^* d_{ij} = \varepsilon. \quad (33)$$

Define

$$\underline{\gamma} := \sum_{i=1}^{|\Xi|} \hat{p}_i \min_{j \in A_i(\lambda^*)} d_{ij}, \quad \bar{\gamma} := \sum_{i=1}^n \hat{p}_i \max_{j \in A_i(\lambda^*)} d_{ij}.$$

By definition, we have

$$\alpha_i^*(\lambda^*) = \max_j \{h(\mathbf{x}, \xi_j) - \lambda^* d_{ij}\},$$

and therefore $\alpha_i^*(\lambda^*) + \lambda^* d_{ij} \geq h(\mathbf{x}, \xi_j)$ for all i, j , with equality if and only if $j \in A_i(\lambda^*)$. Consequently, the complementary slackness condition (32) implies that $j \in A_i(\lambda^*)$ for all $i, j \in \{1, \dots, |\Xi|\}$ such that $\pi_{ij}^* > 0$. Furthermore, since π^* is feasible, it must be true that $\sum_{j=1}^{|\Xi|} \pi_{i,j}^* = \sum_{j \in A_i(\lambda^*)} \pi_{i,j}^* \hat{p}_i$. This implies that

$$\sum_{j \in A_i(\lambda^*)} \pi_{ij}^* d_{ij} \in \left[\hat{p}_i \min_{j \in A_i(\lambda^*)} d_{ij}, \hat{p}_i \max_{j \in A_i(\lambda^*)} d_{ij} \right],$$

and hence

$$\underline{\gamma} \leq \sum_{i=1}^{|\Xi|} \sum_{j=1}^{|\Xi|} \pi_{ij}^* d_{ij} \leq \bar{\gamma}. \quad (34)$$

Combining (34) and (33), we find that $\varepsilon \in [\underline{\gamma}, \bar{\gamma}]$.

Now there are two subcases:

- If $\bar{\gamma} = \underline{\gamma}$, then there exists \bar{d} such that $d_{i,j} = \bar{d}$ for all $i \in \{1, \dots, |\Xi|\}$ and $j \in A_i(\lambda^*)$. In such a case, we set $\beta = 0$, whence $\hat{\pi}_{ij} = \hat{p}_i$ if $j = \underline{j}(i)$ and $\hat{\pi}_{i,j} = 0$ otherwise. By construction, $\hat{\pi}_i$ satisfies complementary slackness condition (32) and the constraint $\sum_{i=1}^{|\Xi|} \hat{\pi}_{ij} = \hat{p}_i$. Furthermore,

$$\sum_{i=1}^{|\Xi|} \sum_{j=1}^{|\Xi|} \hat{\pi}_{ij} d_{ij} = \sum_{i=1}^{|\Xi|} \hat{p}_i \bar{d} = \varepsilon,$$

so $\hat{\pi}$ is feasible and satisfies complementary slackness condition (31).

- If $\bar{\gamma} > \underline{\gamma}$, then

$$\beta := \frac{\varepsilon - \underline{\gamma}}{\bar{\gamma} - \underline{\gamma}} \in [0, 1]. \quad (35)$$

Algorithm 3 chooses for each i the indices

$$\underline{j}(i) \in \arg \min_{j \in A_i(\lambda^*)} d_{ij}, \quad \bar{j}(i) \in \arg \max_{j \in A_i(\lambda^*)} d_{ij},$$

and sets

$$\hat{\pi}_{i,\underline{j}(i)} = (1 - \beta)\hat{p}_i, \quad \hat{\pi}_{i,\bar{j}(i)} = \beta\hat{p}_i,$$

Then, by construction, $\hat{\pi}$ satisfies complementary slackness condition (??) and $\sum_j \hat{\pi}_{ij} = \hat{p}_i$ for all i . Furthermore,

$$\begin{aligned} \sum_{i=1}^{|\Xi|} \sum_{j=1}^{|\Xi|} \hat{\pi}_{ij} d_{ij} &= \sum_{i=1}^{|\Xi|} \hat{p}_i \left((1 - \beta)d_{i,\underline{j}(i)} + \beta d_{i,\bar{j}(i)} \right) \\ &= \underline{\gamma} + \beta(\bar{\gamma} - \underline{\gamma}) = \varepsilon, \end{aligned} \quad (36)$$

so $\hat{\pi}$ is feasible and satisfies complementary slackness condition (31).

Case 2: $\lambda^* = 0$. In this case, primal feasibility requires only $\sum_{i,j} \pi_{ij} d_{ij} \leq \varepsilon$. Moreover, for each $i \in \{1, \dots, |\Xi|\}$, we have that $A_i(0) = \arg \max_{j \in \{1, \dots, |\Xi|\}} h(\mathbf{x}, \xi_j)$. Let π^* be a primal optimal solution. Then, by complementary slackness condition (32), it must be true that $j \in A_i(\lambda^*)$ for all $i, j \in \{1, \dots, |\Xi|\}$ such that $\pi_{ij}^* > 0$. Furthermore, the solution π^* is feasible, so

$$\sum_{i=1}^{|\Xi|} \sum_{j \in A_i(0)} \pi_{ij}^* d_{ij} = \sum_{i=1}^{|\Xi|} \sum_{j=1}^{|\Xi|} \pi_{ij}^* d_{ij} \leq \varepsilon. \quad (37)$$

Algorithm 3 chooses for each i

$$\underline{j}(i) \in \arg \min_{j \in A_i(0)} d_{ij},$$

and sets $\hat{\pi}_{i,\underline{j}(i)} = \hat{p}_i$ and $\hat{\pi}_{ij} = 0$ otherwise. By construction, $\hat{\pi}$ satisfies complementary slackness condition (32) and the primal constraint $\sum_{j=1}^{|\Xi|} \pi_{ij} = \hat{p}_i$ for each $i \in \{1, \dots, |\Xi|\}$. In addition, for each $i \in \{1, \dots, |\Xi|\}$,

$$\sum_{j \in A_i(0)} \pi_{ij}^* d_{ij} \geq \left(\min_{j \in A_i(0)} d_{ij} \right) \sum_{j \in A_i(0)} \pi_{ij}^* = \hat{p}_i d_{i,\underline{j}(i)},$$

where the last equality uses the row-sum constraint $\sum_{j=1}^{|\Xi|} \pi_{ij}^* = \hat{p}_i$. Summing over i gives

$$\begin{aligned}
\sum_{i=1}^{|\Xi|} \sum_{j=1}^{|\Xi|} \hat{\pi}_{ij} d_{ij} &= \sum_{i=1}^{|\Xi|} \hat{p}_i d_{i, \underline{j}(i)} \\
&\leq \sum_{i=1}^{|\Xi|} \sum_{j \in A_i(0)} \pi_{ij}^* d_{ij} \\
&\leq \varepsilon
\end{aligned} \tag{38}$$

Thus $\hat{\pi}$ is primal feasible when $\lambda^* = 0$, and complementary slackness condition (31) holds since $\lambda^* = 0$. \square